To appear in: *Engineering Fracture Mechanics*
Version February 2014

Reliability assessment of high cycle fatigue under variable amplitude loading: review and solutions

Alessandra Altamura and Daniel Straub

Engineering Risk Analysis Group, Technische Universität München, Germany

Abstract

In fatigue reliability assessments, the random load process is commonly represented by its marginal distribution (load spectrum) only. However, as shown in this paper, the correlation characteristics of the load process can have a strong influence on the fatigue reliability and should be accounted for. The paper reviews the modeling of random fatigue crack growth under variable amplitude loading for reliability analysis. Solutions for fatigue crack growth evaluation at different levels of detailing are described and a fatigue crack growth and failure evaluation algorithm, based on a discretization of the random stress process, is presented. As an alternative, a mean approximation is described. Finally, effective computational methods for assessing the fatigue reliability under variable amplitude loading are introduced and applied exemplarily to a case study. The solutions are based on the first-order reliability method FORM and the subset simulation. Using a Markov process model of the loads, the influence of different types of service histories is investigated, by varying the correlation length of the stress cycle process. The results show that the correlation length of the load process has significant influence on the resulting reliability; the resulting probability of failure can vary up to several orders of magnitude for the same marginal probability distribution of stress amplitudes. Based on the results of the case study, the influences of the stress process correlation and of the adopted failure criteria on the reliability are discussed. The mean approximation and the random variable model of the random load process are demonstrated to be applicable under specific conditions.

1 Introduction

The reliability of mechanical and structural components subjected to high cycle fatigue can be ensured with a safe-life approach, a damage tolerant design or a fail-safe approach. The safe-life approach requires that the fatigue reliability is sufficiently high over the entire service life, which is typically achieved by ensuring that no or only small crack growth occurs [1]. Damage tolerant design ensures that the component does not fail between inspection intervals with a sufficiently high reliability [2]. The fail-safe approach ensures that damages are limited in case of fatigue failure. In many applications, the fail-safe approach is ruled out, and it is necessary to demonstrate sufficient reliability, with or without inspections. Thereby, the uncertainties in fatigue crack growth must be considered, which are associated with the presence and size of initial flaws or cracks, the mechanical properties of the material, the fatigue crack growth models and its parameters, and the stress sequence. Because of these uncertainties, a deterministic fatigue analysis requires large safety factors and leads to a conservative design. This motivates the use of reliability analysis for the assessment of fatigue reliability.

The reliability of components subjected to high cycle fatigue can be evaluated based on a S–N damage accumulation approach or a fatigue crack growth evaluation approach. The former is based on empirically determined S–N curves and a damage accumulation rule, such as Palmgren-Miner. Its advantages are its simplicity and the fact that material parameters are available in the literature for a range of materials and component designs. Its disadvantages are that the models – due to their empirical nature – cannot be extrapolated beyond the range of experiments, and that the simplified models lead to significant uncertainty in the predictions, thus necessitating large safety margins in the design. Various effects that are known to influence the fatigue life are not commonly included in the damage accumulation approach, including the influence of the sequence of stress ranges on the fatigue life: fatigue failures are more likely if higher stress ranges occur at the beginning of service life and lower stress ranges towards the end, than if they occur in reverse [3]. Such effects can be modeled by a fatigue crack growth evaluation approach, which is based on combining linear-elastic fracture mechanics with crack growth models. This approach, however, has the disadvantage of requiring more detailed model inputs and leads to more demanding computations. This holds in particular when a reliability assessment is performed, requiring stochastic model inputs and advanced computations. As a consequence, in most studies on fatigue reliability using a crack growth approach, the stress amplitudes are either

assumed constant or represented by deterministic block sequences. However, these sequences are not always representative of the random service load history to which structures are subjected.

In this paper, effective computational methods for assessing the fatigue reliability under variable amplitude loading are presented. To provide the reader practical guidance for various types of models, we present solutions for different levels of detailing of the crack growth models, e.g. one- and two-dimensional crack growth models, and different failure criteria. The methods are applied to a case study considering a pressurized tube, which demonstrates that the assumptions on the temporal variability of the loading can lead to differences in the probability of failure of up to several orders of magnitude. The common assumptions of constant amplitude loading or block sequences are shown to be potentially non-conservative.

The crack growth models considered in this paper do not explicitly include retardation and acceleration effects due to load interaction. These effects can be included, but some of the computationally efficient procedures presented in this paper are not applicable, resulting in increased computational efforts for problems where retardation and acceleration effects are relevant.

The paper starts out with a detailed introduction to variable amplitude loading. This is followed by a step-by-step introduction to the assessment of fatigue crack growth under variable amplitude loading for various degrees of crack growth model complexity (Section 3). Section 4 summarizes the probabilistic modeling of crack growth and section 5 presents the failure criteria and proposes efficient modeling strategies for these. Section 6 introduces reliability evaluation methods and introduces the algorithms for computing fatigue reliability under variable amplitude loading when fatigue loads are modeled as a Markov random process. Finally, section 7 presents the numerical investigations of the models, which also illustrates the appropriate selection of the presented proposed models and methods under different loading conditions.

2 Variable amplitude loading

2.1 Historical background

Most mechanical and structural components are subjected to variable amplitude loading, also called *spectrum loading* [4], during their service life. In the 1930s, engineers working in aeronautics studied the variable amplitude characteristics of stress cycles in-service.

Measurements of service loads were carried out and the first load spectra were published by Kaul [5]. In 1939, Gassner introduced the first variable amplitude load sequence for testing aeronautical structures [6]. Laboratory experiments require simple load sequences, which however should be representative of the real service conditions. The Eight-Block-Program Test proposed by Gassner is a sequence of loading blocks, now known as "Gassner sequence". Within each block, stress cycles are identical; between blocks, the stress amplitude changes while the mean value remains the same. The lengths of the blocks are defined such that stress amplitudes follow the Lognormal distribution. The Gassner sequence consists of 8 varying blocks, whose sequence is fixed and predetermined. After 8 blocks, the sequence is repeated. This procedure is the core of the "Operational fatigue strength" approach to the design of components under variable amplitude loading [7][8].

With the availability of hydraulic testing machines, more realistic load sequences could be applied for testing. Such load sequences can be derived from experimental measurements. For example, the SAE Fatigue and Evaluation Committee selected test load sequences from existing strain measurements [9][10]. Exhaustive information on fatigue testing under variable amplitude loading can be found in [11], while a review of the standard load sequences used for fatigue testing and on the generation of testing load histories from experimental measurements can be found in [12].

Lardner [13][14][15] and Rau [16] proposed to model variable amplitude loading by random processes. In [13] and [14] an approach for reliability evaluation under random loading is described using the crack propagation law proposed in [17]. Rau [16] describes the fatigue crack growth as a random process, since it is the consequence of the application of random process loads. It is suggested that the propagation of the fatigue crack is independent of the order of application of the stress cycles, when the load is a stationary random process and when a high number of stress cycles is applied, so that variations due to the order of application of the stresses average out.

At the beginning of the 1970s, Schijve investigated the influence of the load sequence on fatigue life [18]. In his study, the effect of the load sequence on crack propagation is investigated by performing experiments applying random loading sequence with short and long blocks of cycles. It was observed that the random load sequences could lead to fatigue lives that differ from those evaluated using laboratory tests with simplified load sequences, demonstrating the importance of

appropriately representing the randomness of fatigue loads. According to [18], "the predicted life does not depend so much on the sequence, provided that it is random in some way or programmed with a short period", which confirms the findings of [16]. However, simplified loading sequences consisting of repeated large blocks may lead to unconservative fatigue life predictions due to sequence effects. Following these studies, the need to account for the stochasticity of fatigue crack growth under variable loading was recognized.

2.2 Fatigue load as a random process

When describing load sequences from experimental load measurements, procedures for identifying load cycles from the stress-time history are necessary [19]. Standardized procedures reported in [4] are: level-crossing counting, peak counting, simple-range counting and rainflow counting. These methods result in a sequence of stress cycles, which are characterized by their stress ranges $\Delta\sigma$ and stress ratios R, or alternatively by their minimum and maximum stresses σ_{min} and σ_{max}. Note that the definition of the ordering in which the sequences occur is not necessarily unique if the stress process is a broad band process [20]. Statistically, the load sequence can be described by the random processes $\{\Delta\sigma(n)\}, \{R(n)\}$, i.e. for every stress cycle n there is a random variable pair $\Delta\sigma(n)$ and $R(n)$. Values of $\Delta\sigma(n)$ and $R(n)$ at different cycles will generally be correlated. We limit the discussion to stationary load processes, since the assumption of stationarity is sufficient for most relevant applications. To ease notation, we drop the index n and denote the processes by $\{\Delta\sigma\}$ and $\{R\}$.

Under the assumption of a Gaussian copula model (also known as the Nataf distribution model [21]), a stationary random process is fully characterized by its marginal distribution and its autocovariance function [22]. These can be determined from observed load sequences. Alternatives are presented by Markov chain models as reported e.g. in [23][24][25][26]. In general, Markov process models – due to their flexibility – can model the real dependence structure among stress cycles with higher accuracy. For example, switching Markov models [24] can well represent different modes of operations of mechanical systems and structures. However, given the uncertainties associated with determining in-service stresses in real structures, the Gaussian copula model will be sufficiently accurate for many engineering applications. It is pointed out that the marginal distribution of the stress ranges $\Delta\sigma$ and stress ratios R is not affected by these modeling assumptions.

A Gaussian copula type model for fatigue load processes, which is simultaneously a Markov process, is described in the following. This model will be applied later for numerical investigations, because it has the advantage that the dependence structure is represented by a single parameter. For simplicity, only the stress range is modeled as a random process $\{\Delta\sigma\}$, the stress ratio R is assumed to be constant. The marginal distribution of $\Delta\sigma(n)$ is defined through its cumulative distribution function CDF $F_{\Delta\sigma}$.

Let $\Delta\sigma(n)$ be defined through a transformation T' from a standard Normal variate $V(n)$ as:

$$\Delta\sigma(n) = T'\big(V(n)\big) = F_{\Delta\sigma}^{-1}\Big(\Phi\big(V(n)\big)\Big), \tag{1}$$

where Φ is the standard Normal *CDF* and $F_{\Delta\sigma}^{-1}$ is the inverse CDF of $\Delta\sigma(n)$. If it is imposed that $V(n_i)$ and $V(n_j)$ have the joint Normal distribution, then the corresponding pair of stress ranges $\Delta\sigma(n_i)$ and $\Delta\sigma\big(n_j\big)$, defined through the transformation in Eq. (1), are said to follow the Gaussian copula.

The autocovariance function of the process $\{\Delta\sigma\}$ is described through a corresponding autocovariance function K_{VV} of the underlying standard Normal process $\{V\}$, which is here assumed to be of the exponential type with correlation length z:

$$K_{VV}(\Delta n) = \mathrm{Cov}[V(n), V(n+\Delta n)] = \exp\left(-\frac{\Delta n}{z}\right). \tag{2}$$

The process $\{\Delta\sigma\}$ does not have the same autocorrelation function as the underlying Gaussian process {V}, however, the difference between the two is generally small. $K_{\Delta\sigma\Delta\sigma}(\Delta n)$ is obtained from $K_{VV}(\Delta n)$ by means of the Rosenblatt transformation [27] or the Nataf transformation [21].

It can be shown that with the exponential autocovariance function (Eq. (2)), the process $\{V\}$ has the Markovian property [28]. Consequently, also the process $\{\Delta\sigma\}$ is a Markov process:

$$F_{\Delta\sigma}[\Delta\sigma(n_i)|\Delta\sigma(n_{i-1}), \Delta\sigma(n_{i-2}), .., \Delta\sigma(n_1)] = F_{\Delta\sigma}[\Delta\sigma(n_i)|\Delta\sigma(n_{i-1})]. \tag{3}$$

With this model, the dependence among individual stress ranges is characterized solely by the correlation length z of Eq. (2). To illustrate the effect of z, Fig. 1 shows three different realizations of stress range processes $\{\Delta\sigma\}$ with identical marginal distribution but varying correlation length. It is pointed out that by varying the correlation length z, the load spectrum is

not changing, i.e. the marginal distribution shown on the left-hand side of Fig. 1 of $\Delta\sigma$ is unaltered. However, the correlation length can have an effect on the distribution of the observed realization. In Fig. 1, the underlying marginal distribution is clearly visible from one realization of the process with $z = 1$, but this is not the case for $z = 500$, where all stress ranges in the considered range $n = \{1, \dots, 500\}$ are highly correlated.

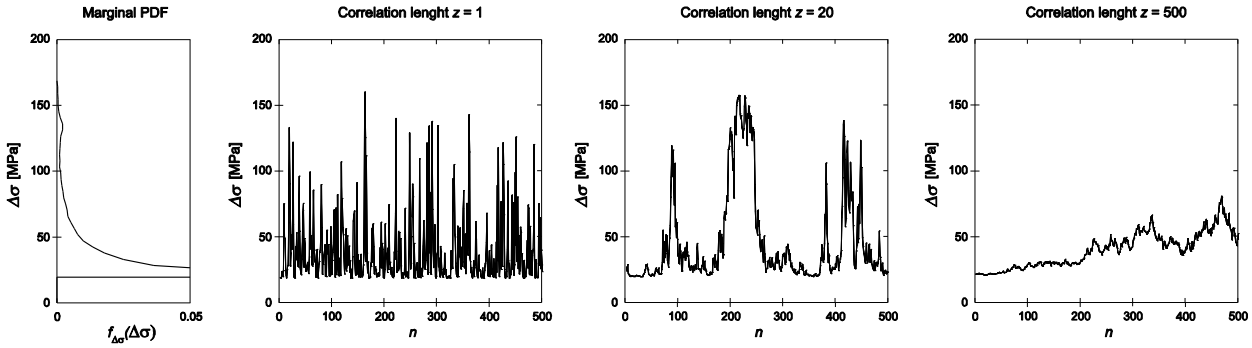

Fig. 1 *Three randomly generated sequences of stress ranges $\Delta\sigma$, whose underlying random processes have identical marginal distribution but varying correlation length z. The marginal distribution of $\Delta\sigma$ is shown on the left-hand side.*

In engineering practice, the marginal distribution of $\Delta\sigma$, i.e. the load spectrum, is often determined from measured load sequences. Thereby, a correct estimation of this distribution is only possible if the measured load sequence is significantly longer than the correlation length. This effect is clearly visible in Fig. 1. In the case of $z = 1$, an empirically determined stress range distribution based on the observed load sequence would be very close to the true underlying marginal distribution shown on the left hand side of Fig. 1. In contrast, for $z = 500$, the observed load sequence clearly is not representative of the true underlying distribution of $\Delta\sigma$. In this case, either a much longer load sequence must be recorded, or several independent shorter load sequences must be recorded, e.g. load sequences arising from different missions, and combined using the total probability theorem. Alternatively, measurements can be combined with or replaced by fatigue load calculations based on statistical models of the load environment, such as for offshore and marine structures subject to wave loads.

2.2.1 Discretization of the fatigue load process into blocks

For practical purposes, it is computationally advantageous to approximate the random load sequence by blocks of cycles with constant amplitude and stress ratio. Such blocks can be defined from the original fatigue load process $\{\Delta\sigma\},\{R\}$ by dividing the sequence of cycles into blocks of b cycles. To each block i, we assign a stress range $\Delta\sigma_i$ and a stress ratio R_i that are equal to the values of the stress cycle at the mid-point of the block $\Delta\sigma_i = \Delta\sigma_{(i-1/2)b}$. Unlike the blocks of the Gassner sequence, or similar deterministic load sequences, the loading blocks obtained with this method still represent a random process. The resulting stress range process has the same marginal distribution $F_{\Delta\sigma}$ as the original one. The average autocovariance function of the block approximation of $\Delta\sigma$ is:

$$K_{\widetilde{\Delta\sigma}\widetilde{\Delta\sigma}}(\Delta n) = K_{\Delta\sigma\Delta\sigma}(k\cdot b) - \frac{\Delta n - k\cdot b}{b}\left[K_{\Delta\sigma\Delta\sigma}(k\cdot b) - K_{\Delta\sigma\Delta\sigma}\big((k+1)\cdot b\big)\right], \tag{4}$$

with

$$k = floor\left(\frac{\Delta n}{b}\right). \tag{5}$$

The error in the covariance is small as long as the correlation length is much larger than the block size, $z \gg b$.

Fig. 2 exemplarily illustrates the stress range block sequence corresponding to the realizations of the stress ranges shown in Fig. 1, with a block length of 25 cycles. It can be observed that the approximation becomes better with increasing correlation length z.

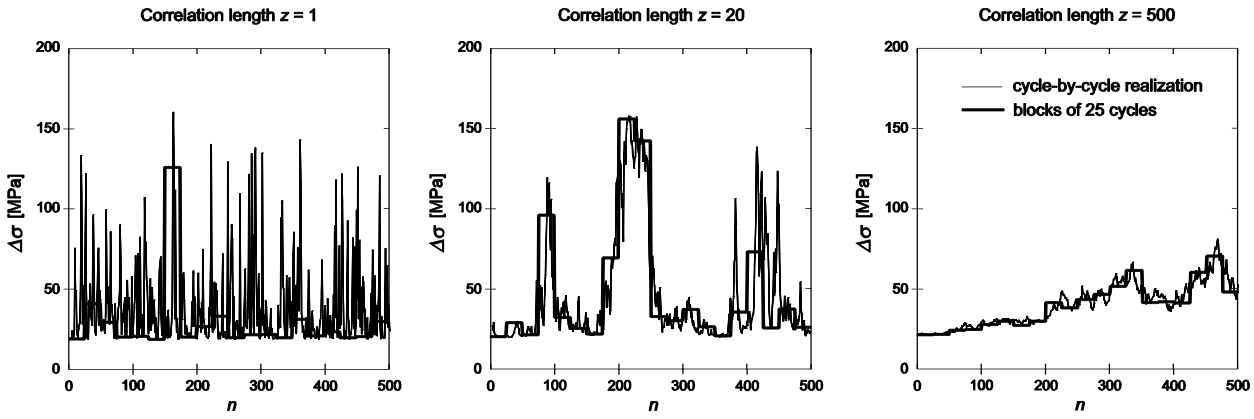

Fig. 2 *Approximated load sequences built as blocks of length 25, superimposed on the load sequences shown in Fig. 1. The value of* Δσ *at each block is equal to the mid-point value of the original random process at each block.*

3 Fatigue crack growth evaluation under constant and variable amplitude loading

3.1 Models of fatigue crack growth

Starting from an initial flaw or notch, cracks will form and grow under cyclic loading. Cracks that grow in two directions usually exhibit a near-elliptical or semi-elliptical shape [29] [30]. Thereby, the crack front advances in all directions, with coordinates x_i, x_j, x_k ..., as depicted in Fig. 3.

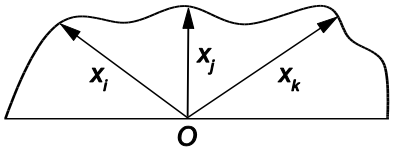

Fig. 3 *Crack with a near semi-elliptical shape and various cracks advance directions, where* O *is the origin.*

Crack growth in any direction x_i is described by a differential equation expressing the crack growth rate $\frac{\mathrm{d}x_i}{\mathrm{d}n}$ as a function of the stress intensity factor range along the crack front in the x_i direction, ΔK_{x_i}:

$$\frac{\mathrm{d}x_i}{\mathrm{d}n} = h_{x_i}\left(\Delta K_{x_i}, R, \delta\right), \tag{6}$$

where R is the stress ratio and δ is a set of parameters related to the material properties. For the case of the Paris law we have $h_{x_i}(\Delta K_{x_i}, \delta) = C \cdot \Delta K_{x_i}^m$ with parameters $\delta = [C, m]$. More advanced models for h_{x_i} include:

- the bilinear crack growth model adopted in BS 7910 [31], [32] , in which the crack growth is described with a Paris model and two different slopes are used to describe the near-threshold region and the Paris region, respectively: $h_{x_i} = C_1 \cdot \Delta K_{x_i}^{m_1}$ and $h_{x_i} = C_2 \cdot \Delta K_{x_i}^{m_2}$ for $\Delta K_{x_i} > \Delta K_{th}$;
- the Forman-Mettu model [33], which is summarized in Annex A, and which is used in the numerical investigations presented later.

When the stress sequence is characterized by overloads, the so-called retardation effect is observed. In the cycles following the overload, a lower crack propagation rate is observed, due to the plasticity induced closure caused by a larger plastic zone that is the result of the overload [34]. Due to this effect, the rate of fatigue crack growth is known to depend on the order in which tensile and compressive overloads are applied [34] and the type of stress sequence has an effect on the fatigue life [35], [36]. Following the observation of crack closure by Elber [37], [38], several models for crack closure were developed to describe the delaying effects of high loads, such as the Wheeler model [39], the Willenborg model [[40], the more realistic strip yield model developed by Newman [41] and the partial crack closure model valid in the near-threshold region [42].

The evaluation of fatigue crack growth requires knowledge of the stress intensity factor ΔK_{x_i} along the entire crack front. A large body of research has focused on deriving analytical or numerical expressions for ΔK_{x_i}, including [29], [43], [44], [45], [46]. For certain geometries, exact analytical solutions or approximate analytical expressions are available, in other cases FEM analysis is necessary, e.g. [47], [48], [49], [50].

If the geometry of the crack is approximated by a perfect semi-elliptical or elliptical shape, then it is fully described by the semi-lengths of the two axes, called a and c, which correspond to the two main growth directions [29], as shown in Fig. 4. In the remainder, we will use this approximation.

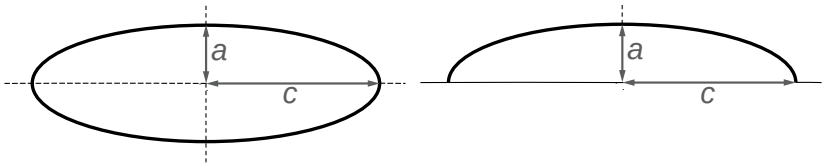

Fig. 4 *Scheme of an elliptical and a semi-elliptical crack with semi-axes a and c, corresponding to the main growth directions.*

The stress intensity factor ranges in the two directions a or c, denoted by ΔK_a and ΔK_c, are a function of the geometry of the component, the crack dimensions a and c, and the applied stress range $\Delta\sigma$. It is distinguished between the membrane stress range, $\Delta\sigma_m$, and the bending stress range, $\Delta\sigma_b$, which varies along the section. In absence of residual stresses, both components can be directly evaluated from a total stress range $\Delta\sigma = \Delta\sigma_m + \max \Delta\sigma_b$ [51]. For ease of presentation, we only consider $\Delta\sigma$. Therefore, we can write the stress intensity factor range in terms of $\Delta K_a = \Delta K_a(a, c, \Delta\sigma, \gamma)$ and $\Delta K_c = \Delta K_c(a, c, \Delta\sigma, \gamma)$ and equation (6) can be rewritten as follows:

$$\frac{\mathrm{d}a}{\mathrm{d}n} = h_a(\Delta K_a(a, c, \Delta\sigma, \gamma), R, \delta), \tag{7}$$

$$\frac{\mathrm{d}c}{\mathrm{d}n} = h_c(\Delta K_c(a, c, \Delta\sigma, \gamma), R, \delta), \tag{8}$$

where:

- $\frac{\mathrm{d}a}{\mathrm{d}n}$ and $\frac{\mathrm{d}c}{\mathrm{d}n}$ are the crack growth rates in directions a and c;
- h_a and h_c are the functions describing the crack growth rate;
- R is the stress ratio;
- δ is a set of parameters describing material properties;
- γ is a set of parameters describing the geometry of the component containing the crack.

It is reminded that h_a and h_c can include threshold effects. If retardation is taken into account, a crack closure model with corresponding parameters has to be included in the crack growth rate equations. In these cases, h_a and h_c are additionally a function of the stresses in previous cycles.

3.2 Evaluation of fatigue crack growth

In the following, the evaluation of one- and two-dimensional crack growth under constant and variable amplitude loading is presented. The parameters R, δ and γ are assumed constant. Generally they may be modeled as deterministic or random variables.

3.2.1 One-dimensional crack growth with constant amplitude loading

For one-dimensional crack growth, the crack is fully characterized by its depth a, as shown in figure 3. Crack growth is thus fully described by Eq. (7).

With constant amplitude, the crack growth can be evaluated from the boundary condition on the initial value of crack depth a_0. By reformulating Eq. (7) and integrating on both sides, one obtains:

$$N = \int_0^N dn = \int_{a_0}^{a} \frac{\mathrm{d}a}{h_a(\Delta K_a(a, \Delta\sigma, \gamma), R, \delta)}, \tag{9}$$

where N is the number of stress cycles to reach a crack depth a.

Eq. (9) can be solved numerically. For special cases, analytical solutions exist, e.g. for the simple Paris law, [19]. If the interest is in finding the crack depth a as a function of the number of stress cycles n, a root finding algorithm can be employed; this algorithm requires evaluating the integral in Eq. (9) for different values of a.

3.2.2 Two-dimensional crack growth with constant amplitude loading

In case of two-dimensional crack growth, the crack is described by its depth a and its width c. Crack growth is described by the two coupled differential equations given in Eq. (7) and (9).

An approximate solution of these coupled differential equations is obtained through a step-wise solution. Let Δn denote the number of cycles in each step. In the i^{th} step, the crack advances from a_i,c_i to a_{i+1},c_{i+1}. If the ratio of crack depth to width is fixed in each step to $\left(\frac{a}{c}\right)_i$, then the two differential equations can be integrated separately, as shown in equations (10) and (11).

$$\Delta n_a = \int_{n_i}^{n_{i+1}=n_i+\Delta n_a} \mathrm{d}n = \int_{a_i}^{a_{i+1}} \frac{\mathrm{d}a}{h_a(\Delta K_a\left(a, \left(\frac{a}{c}\right)_i, \Delta\sigma, \gamma\right), R, \delta)}. \qquad (10)$$

$$\Delta n_c = \int_{n_i}^{n_{i+1}=n_i+\Delta n_c} \mathrm{d}n = \int_{c_i}^{c_{i+1}} \frac{\mathrm{d}c}{h_c(\Delta K_c\left(c, \left(\frac{a}{c}\right)_i, \Delta\sigma, \gamma\right), R, \delta)}. \qquad (11)$$

Note that in the above expressions for the stress intensity factor ranges, the variables a or c respectively have been replaced by the fixed ratio $\left(\frac{a}{c}\right)_i$. I.e., when computing ΔK_a, the value of c is approximated by $a\left(\frac{a}{c}\right)_i^{-1}$, and when computing ΔK_c, the value of a is approximated by $c\left(\frac{a}{c}\right)_i$.

In equations (10) and (11), the integrals are evaluated for fixed values of a_{i+1} and c_{i+1}. In order to find the crack dimensions after Δn cycles, an iterative procedure is required. A root-finding algorithm is employed to find values of a_{i+1} and c_{i+1} that assure $\Delta n_a = \Delta n_c = \Delta n$.

The above is an approximation due to the assumption of a constant ratio $\left(\frac{a}{c}\right)_i$ within a block. An exact solution could only be obtained by cycle-by-cycle evaluation of the increment of a and c, which corresponds to setting $\Delta n = 1$ in equations (10) and (11), with associated large computational efforts. The error of the approximation increases with increasing Δn.

The two-dimensional problem could be simplified and reduced to a one-dimensional problem if $\frac{a}{c}$ were assumed constant throughout the entire process or if a parametric relation between a and c were defined as $c = c(a)$ [52].

3.2.3 One-dimensional crack growth with variable amplitude loading

With random variable amplitude fatigue loading, the stress range $\Delta\sigma$ and the stress ratio R are a function of n. Therefore, Eq. (7) is rewritten to:

$$\frac{\mathrm{d}a}{\mathrm{d}n} = h_a(\Delta K_a(a, \Delta\sigma(n), \gamma), R(n), \delta). \qquad (12)$$

In the following, we first present the evaluation of crack growth described through Eq. (12) for a deterministic realization of the stress process $\{\Delta\sigma\}, \{R\}$. Thereafter, we describe the solution for a random load process $\{\Delta\sigma\}, \{R\}$ through a first-order approximation.

Crack growth evaluation for a deterministic realization of the stress process

For a given realization of the stress process, $\left\{\left(\widehat{\Delta\sigma}(1),\hat{R}(1)\right);\ldots;\left(\widehat{\Delta\sigma}(l),\hat{R}(l)\right);\ldots;\left(\widehat{\Delta\sigma}(N),\hat{R}(N)\right)\right\}$, an exact solution can be obtained through a cycle-by-cycle calculation. Unfortunately, the cycle-by-cycle calculation is computationally expensive for high-cycle fatigue. This holds in particular when the randomness of the stress process must be taken into account.

An approximate solution can be obtained by representing the load sequence with blocks of b cycles with constant stress amplitude and constant stress ratio, as presented in section 0. The crack growth during the ith block Δa_i is now obtained from the solution for constant amplitude loading given in section 3.2.1, i.e. Δa_i is found from the following condition:

$$b = \int_{a_i}^{a_i+\Delta a_i} \frac{\mathrm{d}a}{h_a(\Delta K_a\left(a,\widehat{\Delta\sigma}_i,\gamma\right),\hat{R}_i,\delta)}. \qquad (13)$$

$\widehat{\Delta\sigma}_i$ and $\hat{R}_i$ are the values of the stress process realization at the midpoint of the ith block.

Eq. (13) can be used whenever the load is given as a deterministic sequence of stress ranges and stress ratio values, as for example in [6], [53], [36], [54], [55]. If the stress process is random, Eq. (13) can be used to evaluate the crack growth for realizations of the stress process in a simulation approach, as presented later in this paper. The approach of Eq. (13) is also implemented in the program AFGROW [56]. Note that Eq. (13) is not suitable when retardation effects are important.

Mean approximation to the crack growth evaluation for a random stress process

Crack growth is a cumulative process, in which the contributions of the individual stress cycles are added up. This motivates an approximation of the random crack growth process by the mean crack growth. This approach has been followed by a number of authors, e.g. [32], [57], [76], [77]. The crack growth rate $\frac{\mathrm{d}a}{\mathrm{d}n}$ expressed in equation (12), is approximated by its expected value with respect to $\{\Delta\sigma\}$ and $\{R\}$, where the stress range $\Delta\sigma$ and the stress ratio R can have any positive value:

$$\frac{\mathrm{d}a}{\mathrm{d}n} \approx \mathrm{E}_{\{\Delta\sigma\}\{R\}}[h_a(\Delta K_a(a,\Delta\sigma(n),\gamma),R(n),\delta)] \\ = \int_0^\infty \int_0^\infty h_a(\Delta K_a(a,\Delta\sigma,\gamma),R,\delta) f_{\Delta\sigma,R}(\Delta\sigma,R)\mathrm{d}\Delta\sigma\mathrm{d}R\,, \tag{14}$$

where $f_{\Delta\sigma,R}$ is the joint CDF of $\Delta\sigma(n)$ and $R(n)$.

The expected value of the fatigue crack growth rate $\mathrm{E}_{\{\Delta\sigma\}\{R\}}[h_a(\Delta K_a(a,\Delta\sigma(n),\gamma),R(n),\delta)]$, does not depend on n if the process is stationary. Therefore, for given distribution of $\Delta\sigma(n)$ and $R(n)$, the crack growth becomes a function of a, δ and γ only:

$$\frac{\mathrm{d}a}{\mathrm{d}n} \approx \mathrm{E}_{\{\Delta\sigma\}\{R\}}[h_a(\Delta K_a(a,\Delta\sigma(n),\gamma),R(n),\delta)] = h'_a(a,\delta,\gamma). \tag{15}$$

With the mean approximation, crack growth can be evaluated through a direct integration of equation (9), where h_a is replaced by h'_a.

The validity of the mean approximation is based on the following conditions for the stress process, which are in agreement with the findings of [16]:

- Stationarity: the probability distribution of the stress process does not depend on n.
- Ergodicity: the statistics of the entire process can be deduced from a single realization of the process.
- Sufficiently mixing: the total number of cycles considered N is much larger than the correlation length of the process.

The requirement of a sufficiently mixing stress process will be further substantiated in the numerical investigations presented later in the paper. Note that the mean approximation cannot account for retardation effects.

To illustrate the mean approximation, let us consider the original Paris law, which disregards the stress ratio $R(n)$ and has material parameters $\delta = [C, m]$ and $\gamma = Y$:

$$\frac{\mathrm{d}a}{\mathrm{d}n} = C \cdot \Delta K^m = C \cdot \left(Y(a) \cdot \Delta\sigma(n) \cdot \sqrt{\pi a}\right)^m. \tag{16}$$

Separating the variables and integrating on both sides we obtain:

$$\int_{a_0}^{a} \left(Y(a) \cdot \sqrt{\pi a}\right)^{-m} \mathrm{d}a = C \cdot \int_0^N \Delta\sigma(n)^m \mathrm{d}n. \tag{17}$$

Under the condition that $\{\Delta\sigma\}$ is stationary, ergodic, sufficiently mixing and that N is large, we can approximate the integral over n on the right hand side of Eq. (17) by an integral over $\Delta\sigma(n)$:

$$\int_0^N \Delta\sigma(n)^m \,\mathrm{d}n \approx N \int_0^\infty f_{\Delta\sigma}(\Delta\sigma) \cdot \Delta\sigma(n)^m \,\mathrm{d}\Delta\sigma = N \cdot \mathrm{E}_{\Delta\sigma}[\Delta\sigma(n)^m]. \tag{18}$$

Note that the approximation is exact in the limit as $N \to \infty$ [58].

Inserting this approximation into equation (17) leads to:

$$\int_{a_0}^{a} \left(Y(a) \cdot \sqrt{\pi a}\right)^{-m} \cdot \mathrm{d}a \approx C \cdot N \cdot \mathrm{E}_{\Delta\sigma}[\Delta\sigma(n)^m], \tag{19}$$

and solving for N gives

$$N = \int_{a_0}^{a} \frac{\mathrm{d}a}{C \cdot \left(Y(a) \cdot \sqrt{\pi a}\right)^m \cdot \mathrm{E}_{\Delta\sigma}[\Delta\sigma(n)^m]}. \tag{20}$$

This is equal to the solution of equation (9), where h_a is replaced by the mean approximation h'_a of the crack growth in Eq. (16).

$$\begin{aligned} h'_a &= \mathrm{E}_{\Delta\sigma}\left[C \cdot \left(Y(a) \cdot \Delta\sigma(n) \cdot \sqrt{\pi a}\right)^m\right] \\ &= C \cdot \left(Y(a) \cdot \sqrt{\pi a}\right)^m \cdot \mathrm{E}_{\Delta\sigma}[\Delta\sigma(n)^m]\,. \end{aligned} \tag{21}$$

The quantity $\{\mathrm{E}_{\Delta\sigma}[\Delta\sigma(n)^m]\}^{\frac{1}{m}}$ can be interpreted as an equivalent stress range [59][60].

As shown above, the mean approximation is asymptotically correct as $N \to \infty$ for the case of the Paris law. This is due to the fact that Paris law allows separating the variables a and $\Delta\sigma$ and, therefore, the integration can be performed as in Eq. (17). For the general case of a crack growth law $h_a(\Delta K_a(a, \Delta\sigma(n), \gamma), R(n), \delta)$, this separation is not possible. However, for common crack growth laws, the mean approximation is still reasonably close under the stated conditions. This is also demonstrated by the numerical investigations presented later.

3.2.4 Two-dimensional crack growth with variable amplitude loading

With random variable amplitude fatigue loading, Eqs. (7) and (9), are rewritten to:

$$\frac{\mathrm{d}a}{\mathrm{d}n} = h_a\left(\Delta K_a\left(a, \left(\frac{a}{c}\right), \Delta\sigma(n), \gamma\right), R(n), \delta\right) \tag{22}$$

$$\frac{\mathrm{d}c}{\mathrm{d}n} = h_c\left(\Delta K_c\left(c, \left(\frac{a}{c}\right), \Delta\sigma(n), \gamma\right), R(n), \delta\right). \tag{23}$$

When the load history is given as a realization of a random process, an exact solution can be obtained performing a cycle-by-cycle crack growth evaluation. However, in general this is not practically feasible for reliability analysis. Alternatively, an approximated crack growth evaluation is possible by representing the load sequence with blocks of b cycles with constant stress amplitude and constant stress ratio, in analogy to the solution in equation (13) for the one-dimensional case:

$$b = \int_{a_i}^{a_i+\Delta a_i} \frac{\mathrm{d}a}{h_a(\Delta K_a\left(a, \left(\frac{a}{c}\right)_i, \widehat{\Delta\sigma}_i, \gamma\right), \hat{R}_i, \delta)} \tag{24}$$

$$b = \int_{c_i}^{c_i+\Delta c_i} \frac{\mathrm{d}a}{h_c(\Delta K_c\left(c, \left(\frac{a}{c}\right)_i, \widehat{\Delta\sigma}_i, \gamma\right), \hat{R}_i, \delta)}. \tag{25}$$

Eqs. (24) and (25) must be solved iteratively for Δa_i and Δc_i, respectively, using a root finding algorithm as described earlier.

The approach of Eqs. (24) and (25) is implemented in commercial software such as NASGRO [61] and AFGROW [56], which have been broadly applied, for example in [54], [62], [63], [64].

In analogy to the one-dimensional crack growth model, a mean approximation can be used to compute the crack growth under a random process fatigue load. The fatigue crack growth rate in both directions a and c are approximated by their expected value with respect to the loading process.

$$\frac{\mathrm{d}a}{\mathrm{d}n} \approx \mathrm{E}_{\{\Delta\sigma\}\{R\}}\left[h_a(\Delta K_a\left(a, \left(\frac{a}{c}\right), \Delta\sigma(n), \gamma\right), R(n), \delta)\right] = h'_a(a, \frac{a}{c}, \delta, \gamma) \tag{26}$$

$$\frac{\mathrm{d}c}{\mathrm{d}n} \approx \mathrm{E}_{\{\Delta\sigma\}\{R\}}\left[h_c(\Delta K_c\left(c, \left(\frac{a}{c}\right), \Delta\sigma(n), \gamma\right), R(n), \delta)\right] = h'_c\left(c, \frac{a}{c}, \delta, \gamma\right). \tag{27}$$

Using the mean approximation, the crack growth evaluation is reduced to the problem described in section 3.2.2, where h_a and h_c are replaced by h'_a and h'_c, respectively. The resulting coupled differential equations cannot be solved in one integration step but must be computed for blocks of cycles following equations (10) and (11).

4 Probabilistic fatigue crack growth

So far, we have considered the random nature of fatigue loads, which are ideally modeled as random processes. However, fatigue crack growth involves additional intrinsically random factors and the model parameters are subject to uncertainty. When evaluating the reliability under fatigue crack growth, these random factors and uncertainties must be addressed.

The scatter in fatigue data under deterministic load sequences was discussed as early as 1927 [65], but it was only after the large replicate experiments at constant amplitude loading performed by Virkler [66] that the intrinsic stochasticity of fatigue crack growth was investigated in more details. This intrinsic stochasticity of fatigue crack growth is due to variability of material properties and material inhomogeneities. As observable from the data obtained by Virkler, Fig. 5, two random effects can be distinguished [67]: (a) each curve has an irregular shape (high frequency stochasticity); (b) the mean crack growth curve of each experiment is different (low frequency stochasticity).

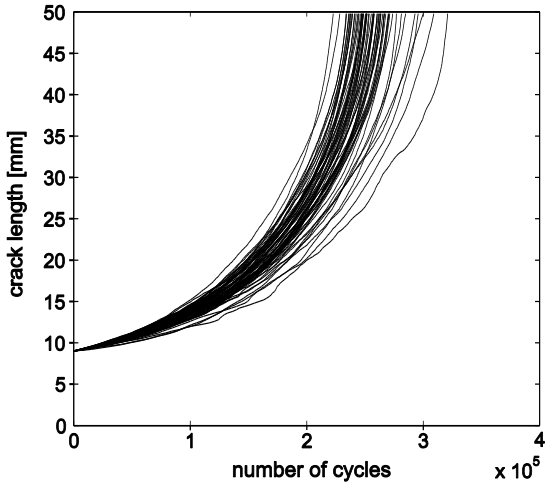

Fig. 5 *Virkler's experiments [66]: crack length versus number of cycles for 68 specimens.*

High frequency stochasticity (a) can be modeled with a *random process approach*, such as the one proposed by [68]. Low frequency stochasticity (b) can be modeled with a random variable approach, i.e. by randomizing the coefficients of the fatigue crack growth law.

In addition to the inherent stochasticity, which can be observed in experiments, the evaluation of fatigue crack growth under service conditions is subject to variability of the loading, as has been addressed earlier, and model uncertainties. The latter can also be tackled by a random variable approach [19].

4.1 Random process approach

Approaches based on random processes have been developed in the 1980s to describe the intrinsic stochasticity of the crack growth observed during large replicate tests with constant amplitude loading, such as those shown in Fig. 5. The aim is to describe the stochasticity of fatigue crack growth under constant or variable loading due to the heterogeneous material structure. The random process model adopted by many authors, e.g. [67] [68] [69] [70] [71] [72] [73] [74] [75], is:

$$\frac{\mathrm{d}x_i}{\mathrm{d}n} = Z(n)h_{x_i}\left(\Delta K_{x_i}, R, \delta\right), \tag{28}$$

where $\{Z(n)\}$ is a random process and x_i is either crack depth a or half-width c. Most authors do not provide a physical interpretation of $\{Z(n)\}$ but its correlation length can be fitted to experimental data [77]. The resulting crack size has the smallest statistical dispersion if $\{Z(n)\}$ is uncorrelated as in [75], and the highest statistical dispersion if $Z(n)$ is fully correlated, in which case the random process reduces to a random variable.

To evaluate the statistics of the crack growth described by Eq. (28), different approaches were proposed in the literature. A Markov process model of the crack growth was proposed in [79], [80] and applied later in [81] [82] [83]. This model was found to provide accurate results for small correlation lengths of the random process $\{Z(n)\}$. However, in [84] it is observed that the best fitting of experimental data is obtained with an intermediate correlation length of $\{Z(n)\}$, provided that the random process model is not combined with a random variable model. Another approach has been proposed by Yang and Manning [68] who demonstrated that if $\{Z(n)\}$ is a lognormal random process and the load is constant, the distribution of crack size can be obtained with a second order approximation. This second order approach has also been used by Wu and Ni [85] to fit experimental data. In [25], a dynamic Bayesian network was applied to assess crack growth described by Eq. (28) conditional on measurement information. Zheng and Ellingwood [86] propose solutions for evaluating the statistics of fatigue crack growth under the random

crack growth described by Eq. (28) as well as under random process loading. For determining the statistics under a random process (variable amplitude) loading, they combine an Euler scheme with Monte Carlo simulation.

It is pointed out that the methods for reliability analysis under variable amplitude loading proposed in this paper are also suitable for crack growth described by Eq. (28). The process $\{Z(n)\}$ can be included in the function h_{x_i} and the procedures presented in Section 3 apply. For the mean approximation to be applicable, the same conditions as stated for the stress range process must also hold for $\{Z(n)\}$. It is noted that the common approach of determining the material parameters from experiments by neglecting the high frequency stochasticity corresponds to an implicit mean approximation.

4.2 Random variable approach

The parameters of the fatigue crack growth models can be represented as random variables [81] [87], [88] [89], [90], [91], [92], [67]. The assumption is that these parameters are random or uncertain but do not vary during the crack growth process. They can represent specimen-to-specimen variability, randomness in the initial condition as well as model uncertainties.

Proper attention has to be paid to the modeling of the correlation among the random variables. As an example, the parameters C and m of Paris' law are highly correlated, and the same holds for most empirically determined material parameters [92], [93].

To obtain the distribution of the crack size for a given number of fatigue cycles, one has to solve functions of random variables. For special, simplified cases, analytical solutions are available [19]. In the general case, numerical solutions are required, such as Monte Carlo simulation or other numerical integration methods.

A complete description of the fatigue crack growth requires a combination of the random variable approach with the random process model. To reproduce the randomness of the crack growth curves shown in Fig. 5, random processes are necessary to represent the variability within each curve and random variables are required to reproduce the observed specimen-to-specimen variability. In principle, the random process model can include the latter as well, by using correlation functions that do approach a non-zero, positive value for values of $n \to \infty$. However, such correlation functions cannot be modeled by Markovian processes and a combined modeling approach is thus preferable. A number of authors have combined the random variable model with

the random process model e.g. [94], [95], [67]. To evaluate the combined model, the statistics of the fatigue crack growth process for given values of the random variables are computed. These conditional statistics must then be integrated over the outcome space of the random variables, using the total probability theorem. Methods for the computation of the reliability for the combined model are introduced in section 6 of this paper.

5 Failure evaluation

When fatigue crack growth evaluation is carried out for reliability assessment, failure criteria have to be defined. In the context of reliability analysis, these criteria are expressed by limit state functions.

5.1 Limit state function

Let **X** denote the set of random variables of the model. A failure event is defined through a limit state function $g(\mathbf{X})$ in such a way that failure occurs when $g(\mathbf{X}) \leq 0$. The probability of failure is thus evaluated as $p_F = \Pr\{g(\mathbf{X}) \leq 0\}$.

In the case of fatigue crack growth, **X** includes the initial crack dimensions a_0 and c_0, the material properties and fatigue crack growth parameters δ, the set of the geometric parameters γ and the applied stress range and stress ratio $\{\Delta\sigma\}, \{R\}$. Furthermore, to make explicit the dependence of the limit state function on the total number of fatigues stress cycles N, the limit state function is written as $g(\mathbf{X}, N) = g(a_o, c_0, \{\Delta\sigma\}, \{R\}, \delta, \gamma, N)$, where a_o, c_0, δ, γ are random variables and $\{\Delta\sigma\}$ and $\{R\}$ are discrete random processes.

In structural reliability, it is convenient to define a failure domain Ω_F in the outcome space of the random variables as

$$\Omega_F(N) = \{g(\boldsymbol{X}, N) \leq 0\}. \tag{29}$$

The probability of failure can then be expressed as a multidimensional integral of the joint probability density function of **X** over the failure domain [19], [96], [97]:

$$p_F(N) = Pr\{g(\boldsymbol{X}, N) \leq 0\} = \int_{\Omega_F(N)} f_{\mathbf{X}}(\mathbf{x})\, \mathrm{d}\mathbf{x}, \tag{30}$$

where $\mathrm{d}\mathbf{x} = \mathrm{d}x_1 \mathrm{d}x_2 \ldots \mathrm{d}x_n$. In general, the solution of this n-dimensional integral cannot be obtained analytically. Structural reliability methods have been especially developed to solve integrals of this form. These methods are adapted for our purposes in section 6.

5.2 Failure criteria

The failure criteria can be of two types:

1. Failure occurs when a critical crack depth, typically the wall thickness, is reached.
2. Failure occurs by plastic collapse or unstable crack growth.

The implementation of the first failure criterion is straightforward, as failure occurs when $a(N) \geq a_{cr}$, where a_{cr} is the critical crack depth. The corresponding limit state function for this failure criterion can be written as:

$$g_1(\mathbf{X}, N) = a_{cr} - a(\mathbf{X}, N). \tag{31}$$

$a(\mathbf{X}, N)$ is the crack depth as evaluated following Section 3.

The second failure criterion includes the two separate failure modes *plastic collapse* and *unstable crack growth*. A well-known approach to represent these two modes is the Failure Assessment Diagram (FAD), also called R6 routine [99], [100]. This approach defines failure in a two-dimensional diagram with a normalized load on the first axis and a normalized stress intensity factor on the second axis. Here, we adopt the crack driving force failure criterion from [51], developed as part of the SINTAP/FITNET procedure [98]. It is based on a separate evaluation of the applied driving force and of the material resistance, leading to a more straightforward evaluation of the factors related to material properties and to applied loads.

The crack driving force failure criterion involves a limit value for the ligament yielding factor ($L_{r,max}$) related to plastic collapse and a limit value for the applied J-integral (J_{mat}) related to unstable crack growth. In the numerical example presented later, the crack driving force failure criterion is applied to longitudinal and radial crack growing directions, which correspond to crack dimensions a and c. The criterion is implemented following [51], using a standard approach for materials not displaying a yield-plateau and applying a plastic correction for the evaluation of $J_{applied}$. Failure occurs when either $J_{applied}(\mathbf{X}, n) \geq J_{mat}$ or $L_r(\mathbf{X}, n) \geq L_{r,max}$ during any cycle n. These two failure modes thus lead to the following two limit state functions:

$$g_2(\mathbf{X}, n) = J_{mat} - J_{applied}(\mathbf{X}, n) \tag{32}$$

$$g_3(\mathbf{X}, n) = L_{r,max} - L_r(\mathbf{X}, n). \tag{33}$$

With random variable amplitude loading, both $J_{applied}(\mathbf{X}, n)$ and $L_r(\mathbf{X}, n)$ become random processes. To assess the crack driving force failure criterion therefore implies the solution of a first passage problem [19]. An exact solution can be obtained only by evaluating the limit state functions at every cycle.

Failure occurs if any of the limit state functions becomes negative. Therefore, combining all failure criteria into a single limit state function gives

$$g(\mathbf{X}, N) = \min[g_1(\mathbf{X}, N), \min_{n=1:N} g_2(\mathbf{X}, n), \min_{n=1:N} g_3(\mathbf{X}, n)]. \tag{34}$$

Alternatively, the limit state function can be expressed in terms of the number of cycles to failure N_{fail}, which can be evaluated with a crack growth algorithm considering the three failure modes defined above. The numbers of cycles to failure for each failure mode are $N_{fail,1}$, $N_{fail,2}$ and $N_{fail,3}$ and are defined as

$$N_{fail,1}(\mathbf{X}) = \min n \quad \text{s.t. } a_{cr} \leq a(\mathbf{X}, n), \tag{35}$$

$$N_{fail,2}(\mathbf{X}) = \min n \quad \text{s.t. } J_{mat} \leq J_{applied}(\mathbf{X}, n), \tag{36}$$

$$N_{fail,3}(\mathbf{X}) = \min n \quad \text{s.t. } L_{r,max} \leq L_r(\mathbf{X}, n), \tag{37}$$

The actual number of cycles to failure N_{fail} is the minimum of the three. The corresponding limit state function becomes

$$g(\mathbf{X}, N) = \min[N_{fail,1}(\mathbf{X}), N_{fail,2}(\mathbf{X}), N_{fail,3}(\mathbf{X})] - N. \tag{38}$$

The limit state functions (34) and (38) are equivalent. However, Eq. (38) has the advantage that the three failure criteria are all expressed in the same unit, the number of cycles. This is

beneficial for most structural reliability methods, as it ensures that the limit state function is not ill-conditioned.

5.3 Numerical evaluation of the limit state function for variable amplitude loading

As pointed out in Section 5.2, under variable amplitude loading, an exact solution requires an evaluation of the failure criteria 2 and 3 at each stress cycle. For most practical problems, an approximate solution is required. In the following, we develop an approximate solution that is based on the block approximation of the random fatigue load process introduced in Section 0. A similar approach is described in [57].

In the block approximation to the fatigue crack growth, (Section 3), the stress range $\Delta\sigma$ and the load ratio R in each block are taken as the midpoint value. This is a reasonable approximation because of the cumulative nature of fatigue crack growth. However, for assessing the failure criteria 2 and 3, it is the maximum stress σ_{max} in each block that is of relevance, which can occur at any cycle within the block. Therefore, the proposed block approximation proceeds by assessing the failure criteria in each block where the applied ligament yielding factor L_r and the applied J-integral are computed with σ_{max}. In each block i, $\sigma_{max,i}$ is a random variable, which is correlated with the midpoint values $\Delta\sigma_i$ and R_i. Unfortunately, an analytical solution for this distribution is not available in the general case. For the special case of no correlation among stress cycles, one can neglect the correlation with the maximum on the midpoint values; the CDF of the maximum stress is then obtained as:

$$F_{\sigma_{max,i}}(\sigma) = [F_{\sigma}(\sigma)]^{b}, \tag{39}$$

where b is the number of cycles in each block.

If the stress cycles are correlated, the distribution of the maximum stress $\sigma_{max,i}$ conditional on the midpoint value σ_i (which is a function of $\Delta\sigma_i$ and R_i) can be evaluated numerically. However, this is a cumbersome procedure.

In many instances, the crack driving force failure criteria are not leading to significantly different results than the critical crack depth criterion. Therefore, a practical solution is to assess the relevance of the crack driving force failure criteria under the assumption of no correlation and under the assumption of constant amplitude loading (full correlation). If the influence of the

crack driving force failure criteria under these two limit cases is found to be small, this indicates that these criteria may be neglected for practical purposes. Otherwise, the evaluation of $F_{\sigma_{max,i}}$ conditional on σ_i is required. This is investigated in the numerical example.

5.4 Proposed algorithm for the evaluation of the limit state function

In practice, direct evaluation of the limit state function (38) can lead to numerical problems. In particular, the number of cycles to failure $N_{fail}(\mathbf{X})$ can become very large or even infinite if the fatigue threshold ΔK_{th} is never exceeded. To remediate these numerical problems, it is convenient to modify the formulation in Eq. (38) to:

$$g(\mathbf{X}, N) = \left\{\min\left[N_{fail,1}(\mathbf{X}), N_{fail,2}(\mathbf{X}), N_{fail,3}(\mathbf{X}), N_{stop}\right] - N\right\} \cdot \{1 - \min[0, (\Delta K_{max} - \Delta K_{th})]\}. \quad (40)$$

Here, N_{stop} is the maximum number of cycles up to which the fatigue crack growth is evaluated. Obviously, it must be $N_{stop} \geq N$. ΔK_{max} is the maximum stress intensity factor in N_{stop} cycles and ΔK_{th} is the fatigue threshold. When using the mean approximation, ΔK_{max} and ΔK_{th} are replaced by their expected values $\mathrm{E}[\Delta K]$ and $\mathrm{E}[\Delta K_{th}]$. The term $\{1 - \min[0, (\Delta K_{max} - \Delta K_{th})]\}$ accounts for the possibility that the fatigue threshold ΔK_{th} is never exceeded and the crack does not propagate. The term has value 1 if crack propagation occurs, and a value larger than 1 when no crack propagation occurs. The term $(\Delta K_{max} - \Delta K_{th})$ ensures that the limit state function is not constant in the non-propagation case and therefore avoids numerical difficulties in structural reliability methods.

In the flow chart of figure Fig. 6, an algorithm for evaluating $N_{min} = \min\left[N_{fail,1}(\mathbf{X}), N_{fail,2}(\mathbf{X}), N_{fail,3}(\mathbf{X}), N_{stop}\right]$ is summarized. This algorithm applies the block approximation of section 3.2.4 for two-dimensional crack growth evaluation under variable amplitude loading.

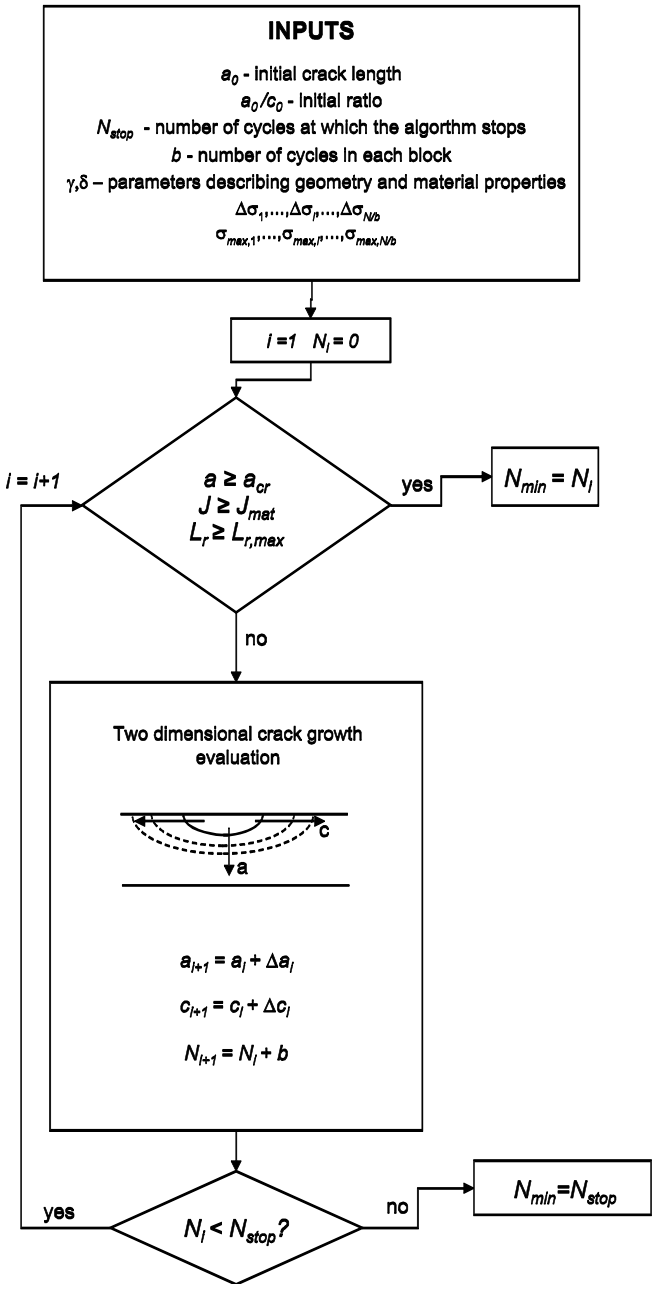

Fig. 6 Flow chart of the algorithm used to evaluate the limit state function defined in equation (40).

6 Reliability evaluation methods

6.1 Generation of a Markov process load sequence for reliability analysis

To solve the structural reliability problem formulated in Eq. (30), the multidimensional integral in the space of **X** is rewritten to an integral in standard normal space:

$$p_F = \int_{\Omega_F(N)} f_{\mathbf{X}}(\mathbf{x})\,\mathrm{d}\mathbf{x} = \int_{G(\mathbf{U},N)\le 0} \varphi_n(\mathbf{u})\mathrm{d}\mathbf{u} = \int_{G(\mathbf{U},N)\le 0} \varphi(u_1)\varphi(u_2)\dots\varphi(u_n)\mathrm{d}u_1\mathrm{d}u_2\dots\mathrm{d}u_n\,, \tag{41}$$

where $\mathbf{U} = [U_1; \dots; U_n]$ are uncorrelated standard normal random variables, φ_n is the n-variate uncorrelated standard normal PDF, and $G(\mathbf{U}, N)$ is the limit state function in the space of U-variables. Underlying Eq. (41) is the equality $\Pr\{g(\mathbf{X}, N) \le 0\} = \Pr\{G(\mathbf{U}, N) \le 0\}$. In order to determine $G(\mathbf{U}, N)$ from $g(\mathbf{X}, N)$, a probability-conserving transformation T from **U** to **X** is required [101], [19], [97]]:

$$G(\mathbf{U}, N) = g(T(\mathbf{U}), N). \tag{42}$$

Due to the large number of random variables used to represent the discrete load process $\Delta\sigma_1, \dots, \Delta\sigma_l$, an efficient procedure is required for this transformation.

The Markovian property of the process $\Delta\sigma_1, \dots, \Delta\sigma_l$ (see Eq. (3)), facilitates the application of the Rosenblatt transformation for this purpose [27]. Thereby, the random variables $U_1, \dots, U_l$ are transformed into the correlated standard normal random variables $V_1, \dots, V_l$ sequentially:

$$V_1 = F_{V_1}^{-1}\big(\Phi(U_1)\big) = U_1, \tag{43}$$

$$V_2 = F_{V_2}^{-1}(\Phi(U_2)|V_1) = \frac{U_2 - \mu_{V_2|V_1}}{\sigma_{V_2|V_1}}, \tag{44}$$

$$V_3 = F_{V_3}^{-1}(\Phi(U_3)|V_2, V_1) = F_{V_3}^{-1}(\Phi(U_3)|V_2) = \frac{U_3 - \mu_{V_3|V_2}}{\sigma_{V_3|V_2}}, \tag{45}$$

$$V_k = \frac{U_k - \mu_{V_k|V_{k-1}}}{\sigma_{V_k|V_{k-1}}}. \tag{46}$$

The conditional mean and standard deviation of V_k given V_{k-1} are:

$$\boldsymbol{\mu_{V_k|V_{k-1}} = V_{k-1}\rho}, \tag{47}$$

$$\sigma_{V_k|V_{k-1}} = \sqrt{1 - \rho^2}, \tag{48}$$

where the correlation coefficient ρ is equal to the covariance between V_{k-1} and V_k, defined following Eq. (2). Due to the stationarity of the load process, ρ is equal for all k. Finally, $\Delta\sigma_1, \dots, \Delta\sigma_l$ are obtained from $V_1, \dots, V_l$ through the marginal transformation defined in Eq. (1).

6.2 Monte Carlo Simulation Method

The Monte Carlo Simulation (MCS) method [101] is generally used for solving multidimensional integrals or integrals for which no analytical solution is available. When solving Eq. (41), MCS consists in generating n_s samples, $\mathbf{u}_i$, $i = 1, \dots i, \dots n_s$, of $\mathbf{U}$, and evaluating the limit state function $G(\mathbf{u}_i)$ for each sample. An estimate of the probability of failure is computed from n_F, the number of samples for which $G(\mathbf{u}_i) \leq 0$, as:

$$p_F \approx \frac{n_F}{n_S}. \tag{49}$$

The MCS method is straightforward to apply, but often requires a significant computational effort, especially when the probability of failure is low. This is due to the fact that the MCS estimate has a coefficient of variation of approximately $\frac{1}{\sqrt{n_s p_F}} = \frac{1}{\sqrt{n_F}}$. As an example, in order to estimate a probability of failure of 10^{-4} with a c.o.v. of 20%, a total of $2.5 \cdot 10^5$ samples are required for each of the random variables.

6.3 First Order Reliability Method

The First Order Reliability Method (FORM) [103] , [101] is an efficient alternative to the MCS method for reliability problems with a limited number of random variables. It utilizes a linear approximation to the limit state function in the space of standard normal random variables **U**. The limit state function is linearized at the so-called design point, $\mathbf{u}^* = [u_1^*; u_2^*; \dots; u_n^*]$, which is point in the failure domain with the highest probability. Sometimes, $\mathbf{u}^*$ is referred to as the most likely failure point, and is obtained by solving the following constrained optimization problem [96]:

$$\begin{aligned} \mathbf{u}^* &= \arg\min \|\mathbf{u}\| \\ &\text{s.t. } G(\mathbf{u}) \leq 0. \end{aligned} \tag{50}$$

$\|\mathbf{u}\|$ is the Euclidian norm of **u**.

The limit state function is linearized at $\mathbf{u}^*$:

$$G'(\boldsymbol{u}) = G(\mathbf{u}^*) + \frac{\partial G(\mathbf{u})}{\partial u_1}\Big|_{\mathbf{u}=\mathbf{u}^*}(u_1 - u_1^*) + \cdots + \frac{\partial G(\mathbf{u})}{\partial u_n}\Big|_{\mathbf{u}=\mathbf{u}^*}(u_n - u_n^*). \tag{51}$$

The probability of failure associated with this linearized limit state function is the FORM approximation, and it is defined entirely by $\|\mathbf{u}^*\|$, as

$$p_F \approx \Pr(G'(\mathbf{U}) \leq 0) = \Phi_{\mathrm{U}}(-\|\mathbf{u}^*\|), \tag{52}$$

Φ_{U} is the standard normal CDF. The FORM reliability index is defined as $\beta_{FORM} = \|\mathbf{u}^*\|$.

FORM facilitates a sensitivity analysis of the random variables **U** or **X**. Sensitivity factors α_i are obtained as the normalized gradient vector at the design point:

$$\alpha_i = \frac{u_i^*}{\|\mathbf{u}^*\|}, \tag{53}$$

The sensitivity factors α_i take values between -1 and 1. The larger their absolute value, the higher the influence on the reliability. Positive values of α_i indicate that an increase in u_i or x_i leads to an increase of the probability of failure, while negative values of α_i are related to a decrease of the probability of failure for an increasing u_i or x_i.

FORM is computationally efficient in low dimensions, but can become cumbersome and inefficient with increasing number of random variables, due to the optimization problem in Eq. (50). For this reason, FORM is not practical when modeling the fatigue load as a random process, which involves a large number of random variables. It is however applicable in combination with the mean approximation approach.

6.4 Subset simulation

The subset simulation method [104] is a technique based on MCS, which can be used to efficiently evaluate small probabilities of failure in problems involving a large number of random variables.

In subset simulation, intermediate failure events $E_i = \{G(\boldsymbol{U}) \leq o_i\}, i = 1, \ldots, B$, are defined. By requiring $o_1 > o_2 > \cdots > o_B = 0$, it holds $E_1 \supset E_2 \supset \ldots \supset E_B = F$, i.e. E_i is a subset of E_{i-1}, which in turn is a subset of E_{i-2} and so on. The probability of failure can be expressed as:

$$\begin{aligned} p_F &= \Pr\left(\bigcap_{i=1}^{B} E_i\right) \\ &= \Pr(E_B|E_{B-1}) \Pr\left(\bigcap_{i=1}^{B-1} E_i\right) \\ &= \Pr(E_1) \prod_{i=2}^{B} \Pr(E_i|E_{i-1}), \end{aligned} \tag{54}$$

where $\Pr(E_i|E_{i-1})$ is the conditional probability of E_i given E_{i-1}. The samples required to estimate the conditional probabilities $P(E_i|E_{i-i})$ are obtained by means of a Markov Chain Monte Carlo (MCMC) sampling approach using the modified Metropolis-Hastings (M-H) algorithm from [104]. This algorithm allows to generate samples from the conditional distribution of $\mathbf{U}$ given E_{i-1}, $F(\mathbf{U}|E_{i-1})$. The conditional probability $P(E_i|E_{i-1})$ is then evaluated from these samples using a Monte Carlo approach.

The constants o_i are selected so that the probabilities $\Pr(E_i|E_{i-1})$ are large, typically around 0.1. Therefore, the number of samples required for computing each conditional probability is relatively small, typically around 500. Furthermore, the required number of samples increases only linearly with a decrease in the order of magnitude of the probability of failure.

7 Numerical investigation

7.1 Case study

Bi-dimensional fatigue crack growth of a semi-elliptical surface crack in a cold-drawn steel tube subjected to variable amplitude internal pressure is studied. Fig. 7 shows the transversal and longitudinal sections of the tube. The initial flaws are oriented in the longitudinal direction on the external surface of the tube. The tube is of grade E355SR according to the standard EN10305-1 [107] and is produced according to EN10297-1 [108], presenting a ferritic pearlitic microstructure. This case study was subject to a previous numerical and experimental investigation reported in [55].

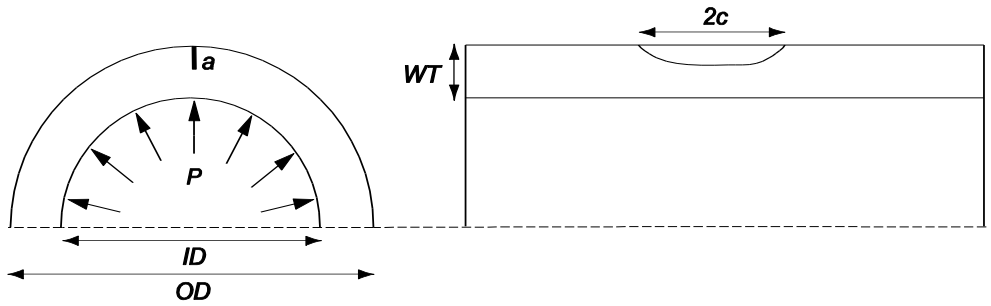

Fig. 7 *Transversal and longitudinal sections of the tube subjected to internal pressure P. On the external surface an initial flaw characterized by the depth a and the semi-length c is present. The geometry of the tube is described by the outer diameter OD, the wall thickness WT, and the inner diameter ID.*

7.2 Structural integrity model, fatigue crack growth equation and failure criteria

For the evaluation of the stress intensity factor and the failure criteria, the model of a semi-elliptical surface crack in a flat plate subjected to pure tension stress is adopted, following [55]. This model is valid for thin-walled thickness tubes and accounts only for the membrane component of the stress σ_m, ignoring the bending component. When applied to thick-walled pipes it provides conservative but reasonable results, in good agreement with experimental observations [55]. The stress intensity factor for this model is evaluated according to [29][105].

The bi-dimensional crack growth is evaluated applying equations (24) and (25), with block cycle length $b = 10^4$ for the discretization of the random stress process. The fatigue crack growth rate

h_a and h_c are expressed through the Forman-Mettu crack growth model, which is summarized in Annex A. This model does not include retardation effects. The failure criteria are implemented following section 5.2 according to the solution given in [51].

Initial flaws with a depth of more than 0.2 mm can propagate under the applied stress sequences. Such surface flaws behave like long cracks, therefore the initiation stage and the small and short cracks behavior can be neglected. This can be seen from the Kitagawa diagram of the material analyzed in this work, as reported in [106].The mechanical and fatigue properties of the considered tube are summarized in Table 1.

Table 1. Mechanical and fatigue properties.

Parameter		**Value**
Monotonic yield stress	σ_y	590 MPa
Cyclic yield stress	$\sigma_{y,cycl}$	350 MPa
Ultimate tensile strength	σ_{UTS}	705 Mpa
Young's modulus	E	210.000 MPa
Poisson's ratio	ν	0.3
Coefficients of the Forman-Mettu model	C_{th}	0.48
	C	$1.33\ 10^{-11}$ MPa√m given da/dN in mm/cycle
	m	2.85
	p	0.3
Fatigue threshold at $R = 0$	$\Delta K_{th,0}$	See Table 2
Fracture toughness	K_{mat}	

7.3 Probabilistic model

The case study includes a number of stochastic variables. Material properties $\Delta K_{th,0}$ and K_{mat} as well as the initial crack size are modeled as random variables; the stress ranges are modeled as a random process. With the applied Forman-Mettu model, the crack growth rate is influenced by the threshold $\Delta K_{th,0}$, and it was found in [55] that the randomness in the fatigue crack growth rate is therefore fully described by the randomness of $\Delta K_{th,0}$. This explains the deterministic values for C and m in the model.

The considered tubes are subjected to non-destructive tests prior to installation. Only tubes without identified flaws are put in service. Therefore, when modeling the size of the initial flaw, the probability of detection POD of the non-destructive test is taken into account. According to Bayes' rule, the posterior PDF of a_0 after the test $f''(a_0)$ can be evaluated from the prior PDF $f'(a_0)$ and from the probability of detection $POD(a_0)$ as [55]:

$$f''(a_0) = \frac{f'(a_0)[1 - POD(a_0)]}{\int_0^\infty f'(a_0)[1 - POD(a_0)]da_0} \tag{55}$$

The POD is defined through a lognormal CDF, $POD(a_0) = \Phi\left(\frac{\ln(a_0)-\theta}{\zeta}\right)$, with parameters $\zeta = 0.32$ and $\theta = -0.56$.

The effect of the non-destructive test on the probability distribution of a_0 is shown in Fig. 8. The model considers only a single surface flaw, which is the one from which the critical crack will grow.

The probabilistic models of the input random variables are summarized in Table 2. The models are based on experimental data reported in [55].

Table 2. Input random variables: distribution and parameters.

Parameters	Distribution	Distribution parameters
K_{mat}	3-parameter Weibull $F(K_{mat}) = 1 - exp\left\{-\left[\frac{(K_{mat} - K_{min})}{(K_0 - K_{min})}\right]^k\right\}$	$K_0 =$ 40 MPa$\sqrt{\text{m}}$, $k = 5$ $Kmin = 28.7\ MPa\sqrt{m}$,
$\Delta K_{th,0}$	Gaussian	$mean = 5.5\ MPa\sqrt{m}$, $stand.dev. = 0.17$
initial flaw depth, a_0	Gumbel type I distribution	see Fig. 8
initial ratio $\frac{a_0}{c_0}$	deterministic	0.1

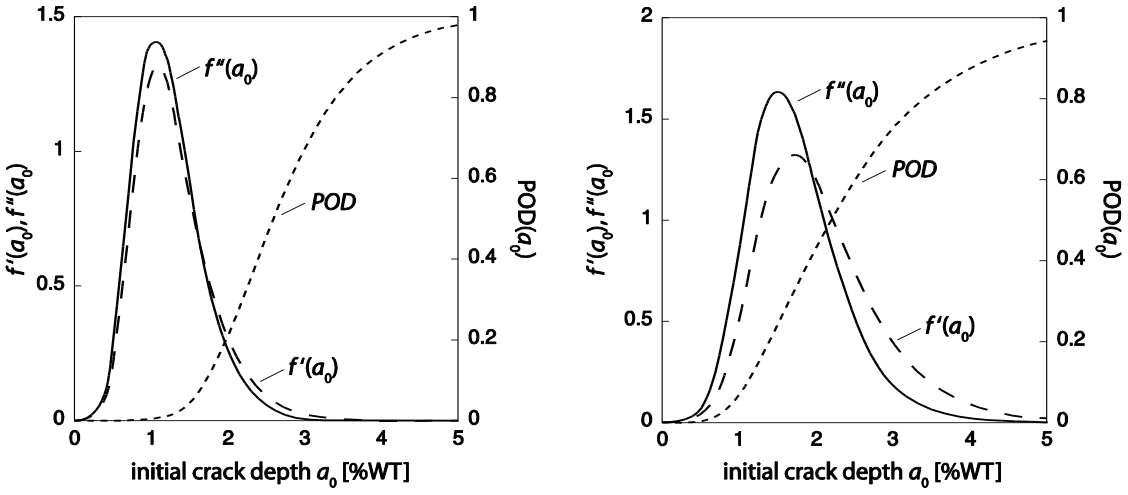

Fig. 8 *Initial flaw depth distribution and updating following non-destructive tests. a_0 is expressed as percentage of the wall thickness for the specific cases of OD=22 mm (left) and OD=14 mm (right), corresponding to case studies C1 and C2 respectively (adapted from [55]).*

7.3.1 Variable stress range processes

The stress ranges are modeled as a Markov process. It is of the Gaussian copula type as described in section 2.2 and is characterized by its CDF $F_{\Delta\sigma}(\Delta\sigma)$ and the autocovariance function (Eq. (2)) with correlation length z. The load ratio is held constant with value $R = 0.1$

Three $F_{\Delta\sigma}(\Delta\sigma)$ are considered: two empirical (C1 and C2) and one analytical CDF (CW), which are depicted in Fig. 9 and summarized in Table 3. C1 and C2 are obtained from service stress measurements on hydraulic cylinders of earth moving machines [55]. CW is a 3-parameters Weibull with the same mean and standard deviation as C1 and is included for comparison. The upper limits of C1 and C2 are justified by safety valves that prevent higher pressures. The uncertainty on these maximum pressures is here neglected.

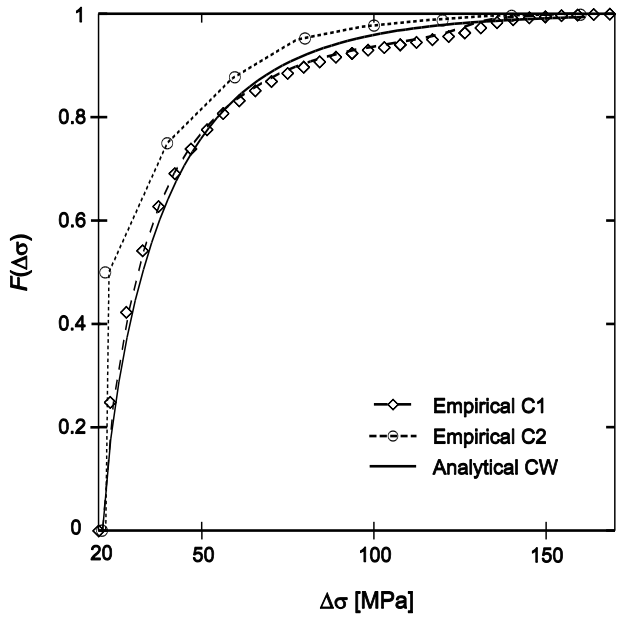

Fig. 9 CDF of the stress range $\Delta\sigma$: two empirical CDFs for the two measured loading processes (empirical C1 and C2), analytical 3-parameters Weibull CDF with the same mean and standard deviation as the empirical C1 (analytical CW).

Table 3. Properties of the three applied load models.

	C1	**C2**	**CW**
Upper limit of the stress range $\Delta\sigma_{UL}$ [MPa]	84	110	∞
Number of stress cycles during service N	$1.8\ 10^7$	$2\ 10^7$	$1.8\ 10^7$
Stress amplitude mean μ_{σ_a} [MPa]	42	34	42
Stress amplitude standard deviation σ_{σ_a} [MPa]	28	23	28

7.4 Reliability evaluation

Three approaches to the reliability evaluation are implemented, which correspond to different models of the stress range process:

Random process approach (RP): The load is modeled as a Markov process (see section 2.2 and 6.1) with various correlation lengths ($z = 1{,}10^3, 10^5, 10^7, 10^9$ cycles) and the reliability is evaluated with a subset simulation algorithm SuS (section 6.4). In the implemented algorithm, the constants o_i defining the intermediate failure events are chosen such that $P(E_i|E_{i-1}) = 10^{-1}$,

and 500 samples are generated at each intermediate simulation step. The load sequences are generated applying the method proposed in section 6.1.

Random variable approach (RV): The load is modeled as a random variable and the first order reliability method (FORM, see section 6.3) as well as MCS (section 6.2) are applied. Modeling the load as a random variable is equivalent to a Markov process with infinite correlation length $z = \infty$, i.e. the stress ranges are constant during the service life of the component.

Mean approximation approach (MA): The mean approximation is applied (section 3.2.3 and 3.2.4) and the reliability is evaluated with FORM. Since the mean approximation does not consider interdependency among stress cycles, it is equivalent to a random process with correlation length zero, $z = 0$.

7.5 Results for the critical crack size failure criterion

In this section, the results obtained for the critical crack size failure criterion are reported. The results obtained when considering also the crack driving force failure criteria are presented in Section 7.6.

Fig. 10 shows the plots of the probability of failure p_F versus the correlation length z of the stress range process $\{\Delta\sigma\}$ for the cases C1, C2, CW and for the different reliability evaluation approaches RP, RV and MA.

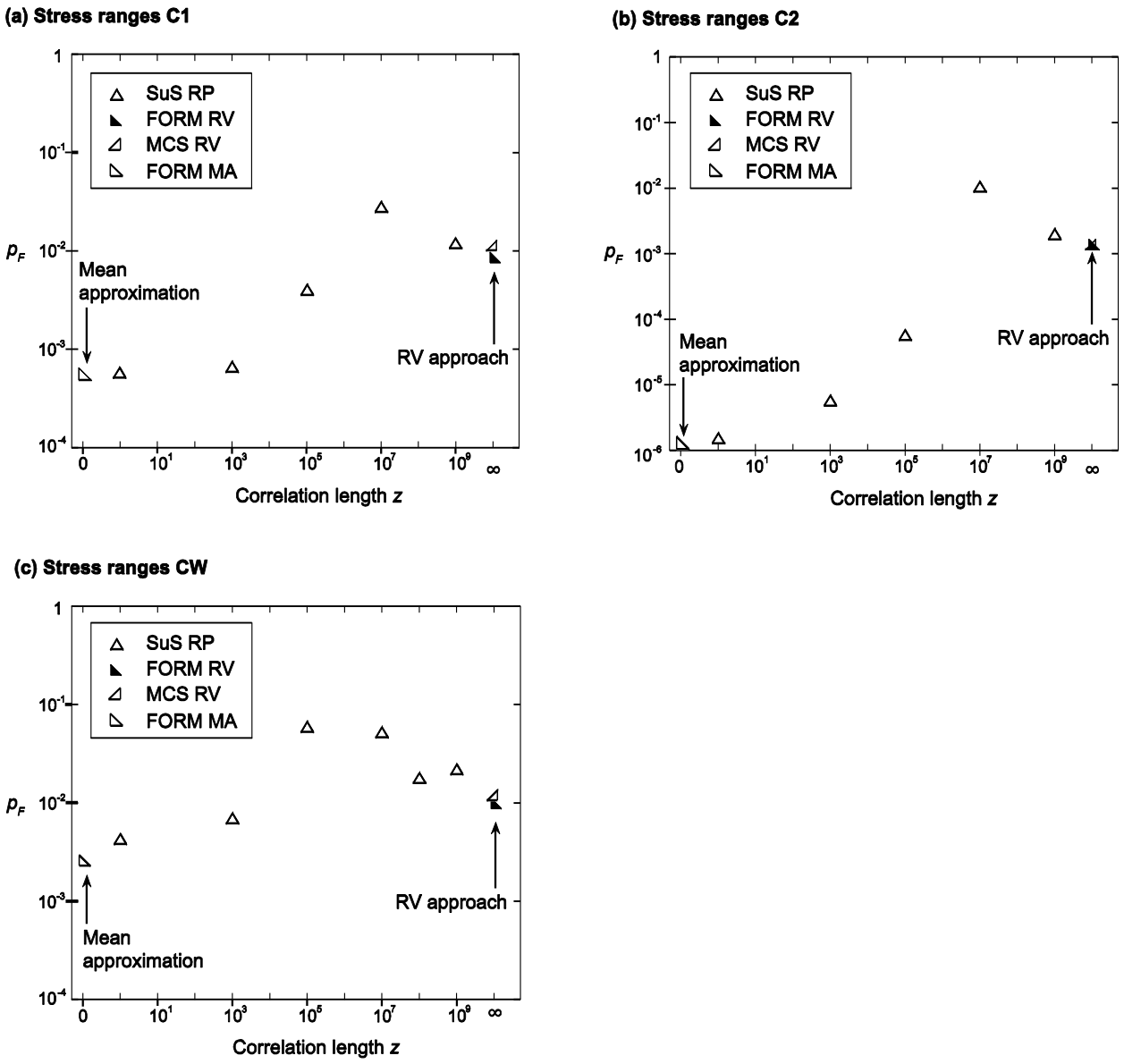

Fig. 10 *Probability of failure p_F versus correlation length z of the stress range process for the three cases: (a) C1, (b) C2, (c) CW. Results for $z = 1{,}10^3, 10^5, 10^7, 10^9$ are obtained describing the load as Markov random process and applying a subset simulation algorithm (SuS RP). Results for $z = \infty$ refer to the case of the load described as a random variable and solved with Monte Carlo simulation or with first order reliability method (MCS RV and FORM RV). Results for $z = 0$ are obtained applying the mean approximation with respect to the stress process and solving with FORM (FORM MA).*

It can be observed from Fig. 10 that the correlation length z of the stress range process has a strong effect on the resulting reliability. In case C2, which is the one with the highest reliability, the probability of failure varies by four orders of magnitude, from 10^{-6} to 10^{-2}. The highest probability of failure p_F occurs for values of z close to the service life time, which is around $2 \cdot 10^7$. For $z > 10^7$, p_F decreases again until it reaches the value corresponding to the random variable case ($z = \infty$). Values of z in the range $10^6 - 10^7$ correspond to cases with a few distinct service conditions during the service life, that is to situations where the stress ranges are similar for longer periods. These are the most unfavorable conditions, since they imply a high probability of enduring a high load level during an extended time period. Shorter correlation lengths correspond to a single service condition with randomly varying stress ranges. In these cases, lower failure probabilities are observed because the mixing of the stress ranges decreases the actual uncertainty in the loading (law of large numbers), that is on average the crack growth rate is lower because of the mixes sequence of high and low stress ranges. Finally, for $z > 10^7$, the probability of having a high load level during lifetime decreases, and therefore the probability of failure slightly decreases.

There is good agreement between the results obtained for a random process model of the stress ranges with a high correlation length ($z = 10^9$) and those obtained by applying the random variable approach. The probability of failure calculated with the mean approximation is close to the one obtained with the load modeled as a random process with a short correlation length ($z = 1$). It should be noted that the correlation length $z = 1$ refers to the specification of the stress process; however, due to the block approximation in the fatigue crack growth evaluation, the correlation length of the simulated stress process is larger than the specified $z = 1$ (see the comments in section 0). This effect is relevant only for the small correlation lengths, i.e. $z = 1$ and $z = 10^3$. It can also explain the slight difference in Fig. 10c between the p_F calculated with the mean approximation and with a random process with correlation length $z = 1$.

The probability of failure of case CW is higher than that of C1, even though the two correspond to stress range processes with the same mean and standard deviation. The difference between the results can be explained by the fact that in the case of CW the distribution of the stress ranges is analytically defined and has no upper limit, which implies a heavier tail of the distribution.

The effect of the two different distribution forms can also be observed in Fig. 11, which compares the mean approximation for cases C1 and CW. Fig. 11a shows the expected value of

the fatigue crack growth rate $\mathrm{E}\left[\frac{\mathrm{d}a}{\mathrm{d}n}\right] = h'_a\left(a, \frac{a}{c}, \delta, \gamma\right)$, Eq. (26), as a function of the crack length, a (see section 3.2.4). The expected value of the fatigue crack growth rate evaluated with CW is slightly higher than that evaluated with C1. Fig. 11b shows the crack depth, a, versus the number of fatigue cycles n when applying the mean approximations shown in Fig. 11a at the design point $\mathbf{u}^*$ of the FORM solution of case C1. It is observed that the analytical Weibull distribution CW leads to a lower number of cycles to failure, which is in agreement with the differences in the probabilities of failure observed between Fig. 10a and Fig. 10c.

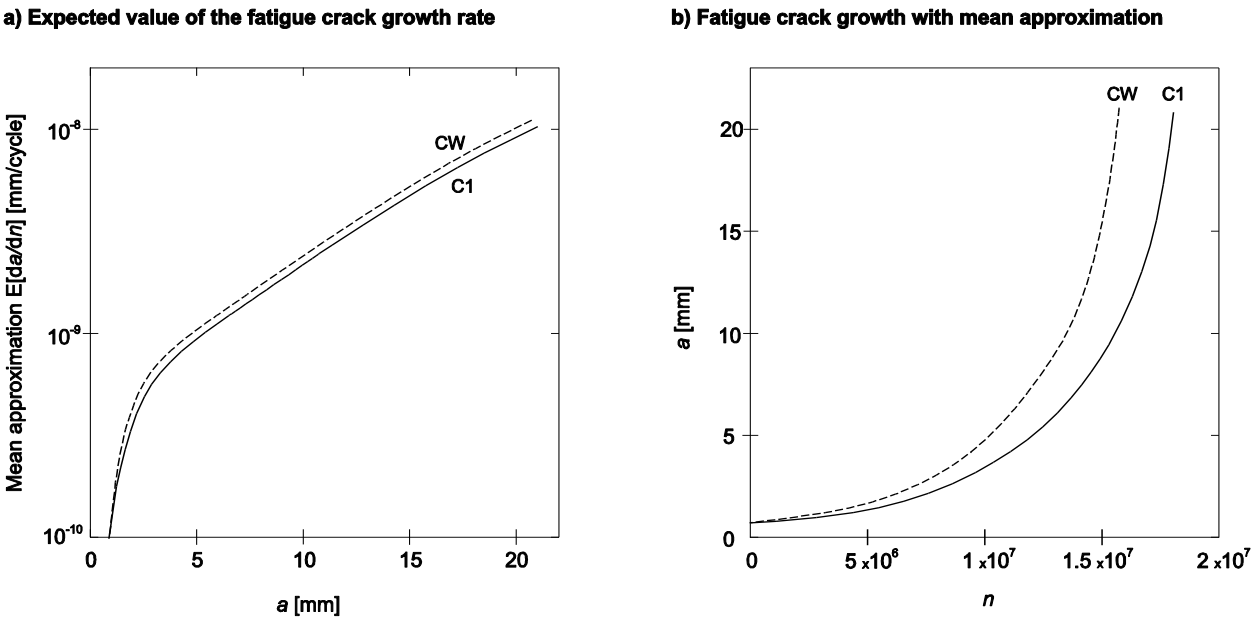

Fig. 11 *Mean approximation for cases C1 and CW: (a) expected value of the fatigue crack growth rate* $\mathrm{E}\left[\frac{\mathrm{d}a}{\mathrm{d}n}\right] = h'_a\left(a, \frac{a}{c}, \delta, \gamma\right)$ *as a function of the crack depth a; (b) crack depth, a, versus the number of fatigue cylcles, n, calculated with the mean approximation at the design point* $\mathbf{u}^*$ *of load case C1.*

Fig. 10 shows that the correlation of the load sequence has a significant influence on the fatigue reliability. To better understand the reasons for this effect, it is helpful to look at some realizations of the crack growth process for different values of the correlation length z. In Fig. 12a, random realizations of the crack growth with a stress range correlation length $z = 1$ are shown for two different values of the initial crack size a_0. In Fig. 12b, random realizations of the

crack growth are shown for the case where the stress range is a random variable ($z = \infty$). Comparing the results for $z = 1$ and $z = \infty$ shows the effect of a small correlation length: the randomness of the stress range process essentially disappears due to the law of large numbers. The differences among the crack growth curves are mainly due to random differences in the initial crack size. Therefore, the resulting randomness is much smaller in this case, and the reliability is significantly higher. This is also confirmed by FORM sensitivity results shown later.

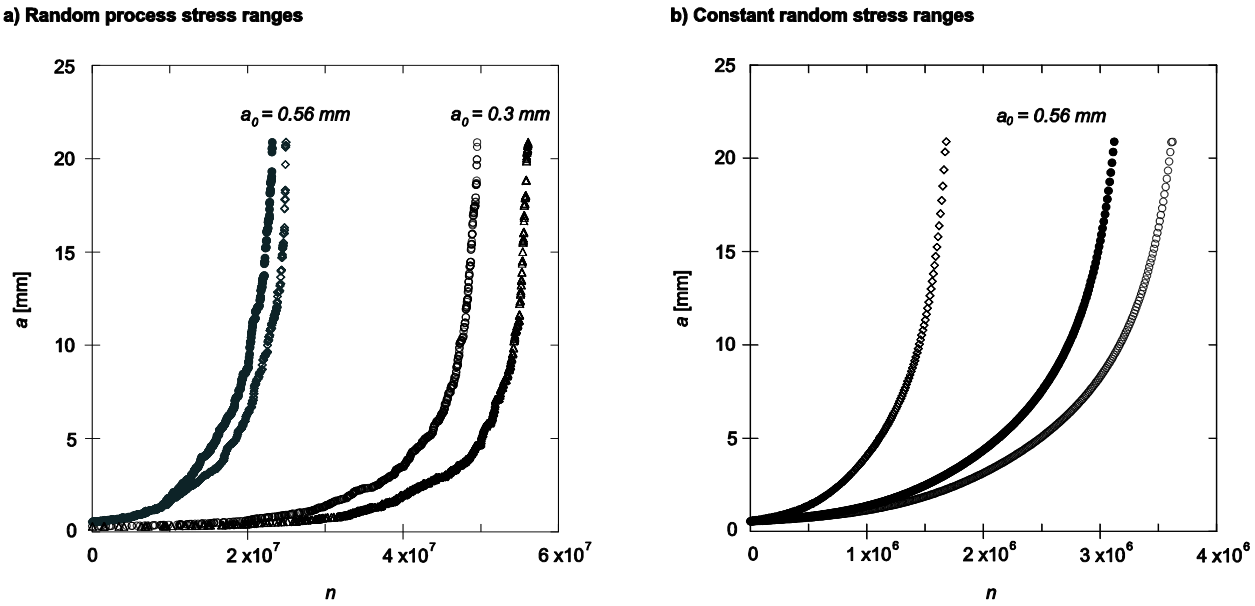

Fig. 12 *Crack depth versus number of cycles for the stress case C1. The crack growth is evaluated: (a) modeling the stress ranges as a random process with correlation length* $z = 1$ *and for two different values of the initial crack depth* $a_0 = 0.3$ *and* $a_0 = 0.56$ *; (b) for random constant stress ranges* ($z = \infty$) *with initial crack depth* $a_0 = 0.56$.

In Fig. 13, random realizations of the crack growth are shown for correlation length $z = 10^7$, together with the underlying load sequences. This value of z is of the same order of magnitude as the service life, and it is the value with the highest failure probability (Fig. 10). It can be clearly observed how the stress range processes correspond to a few distinct service conditions during the service life. This implies a high probability of enduring a high stress range level during an extended time period, which leads to fast crack growth.

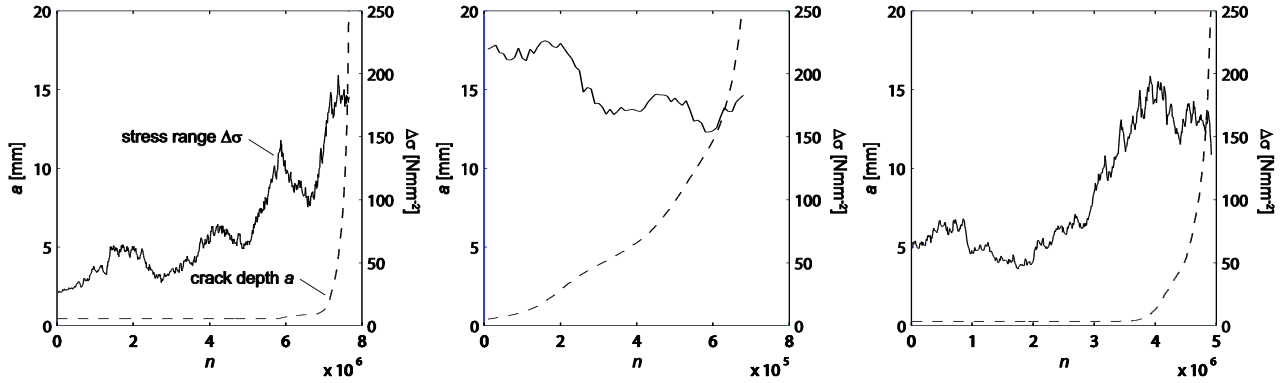

Fig. 13 *Crack depth (dashed) and stress ranges versus number of cycles for three random realizations of stress range processes with correlation length* $z = 10^7$ *based on case CW.*

7.5.1 FORM sensitivity analysis

The FORM algorithm provides sensitivity factors α_i that describe the influences of the random variables on the failure probability (Section 6.3). Table 4 and Table 5 show the FORM sensitivity factors α_i for the random variable approach (corresponding to $z = \infty$) and the mean approximation approach (corresponding to $z = 0$). With the random variable approach, the most influential random variables are the stress range $\Delta\sigma$ and the initial crack depth a_0; the fatigue threshold $\Delta K_{th,0}$ has little influence on the reliability due to its small coefficient of variation (see Table 2). The negative sign of $\alpha_{\Delta K_{th}}$ indicates that a decrease in the value of ΔK_{th} leads to a decrease in reliability. With the mean approximation approach, the only two random variables are $\Delta K_{th,0}$ and the initial crack depth a_0. As can be seen in Table 5, the reliability is determined by the latter.

Table 4. FORM sensitivity analysis for the random variable approach

	C1	C2	CW
$\alpha_{\Delta\sigma}$	0.83	0.89	0.72
$\alpha_{\Delta K_{th,0}}$	-0.04	0.00	-0.04
α_{a_0}	0.56	0.44	0.68

Table 5. FORM sensitivity analysis for the mean approximation approach

	C1	C2	CW
$\alpha_{\Delta K_{th,0}}$	-0.18	-0.03	-0.04
α_{a_0}	0.98	0.99	0.99

7.6 Results - Critical crack size failure criteria and crack driving force failure criteria

Following Section 5.3, the crack driving force failure criteria are evaluated for the two limit cases:

RV: The stress range is a random variable ($z = \infty$, assumption of full correlation);

RP: The stress range is a random process with correlation length $z = 1$ (assumption of no correlation).

The reliability computations are performed with a block size of $b = 10^4$. For the RP case, the CDF of $\sigma_{max,i}$, the maximum stress during b cycles, is evaluated following Eq. (39), and shown in Fig. 14 together with the CDF for case RV. In the latter case, the maximum stress is constant throughout the entire service life and the CDF of $\sigma_{max,i}$, is independent of b. For load models C1 and C2, the maximum stress in RP case is essentially equal to the upper limit of the stress distribution σ_{UL}, as reported in Table 3. For load model CW, where stress ranges follow the Weibull distribution, the stress distribution has no upper limit and high values of $\sigma_{max,i}$ are expected.

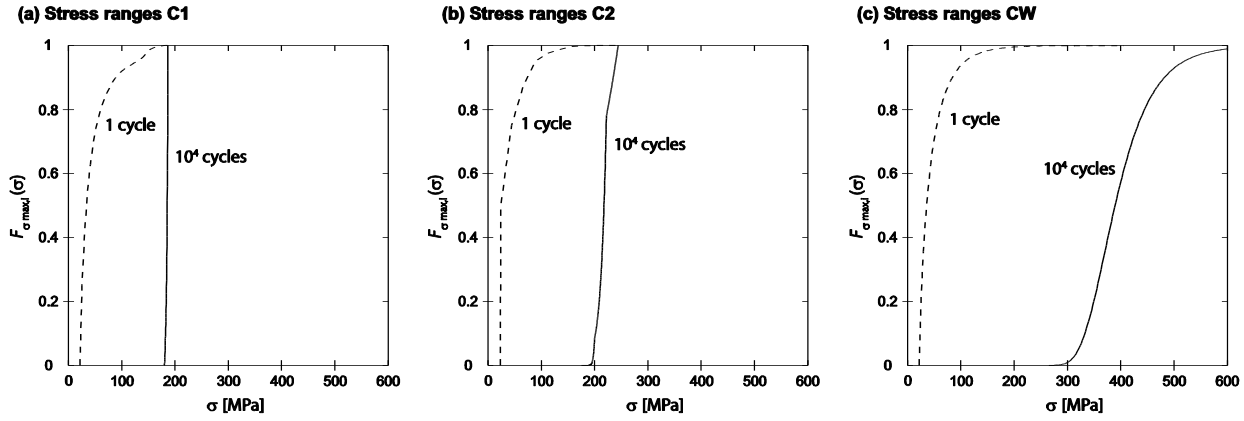

Fig. 14 *CDF of the maximum stress in* $b = 10^4$ *cycles for the three different load cases: (a) C1, (b) C2 and (c) CW.*

Fig. 15 shows the probability of failure p_F versus the correlation length z calculated by applying either the critical crack size failure criterion alone or in combination with the crack driving force failure criteria. The results show that among the investigated cases, the crack driving force failure criteria have a significant influence on the reliability only for load model CW and no correlation ($z = 1$). In this case, the probability of failure is close to one, which is not surprising when looking at the CDF of $\sigma_{max,i}$ in Fig. 14c. Since a total of over 10^3 load blocks occur during the service life, these maximum stresses would lead to failure with high probability even without the presence of a crack. In all other cases shown in Fig. 15, the reliability is only slightly influenced by the crack driving force failure criteria. For $z = \infty$ there is no effect (the differences are due to the randomness of the MCS results).

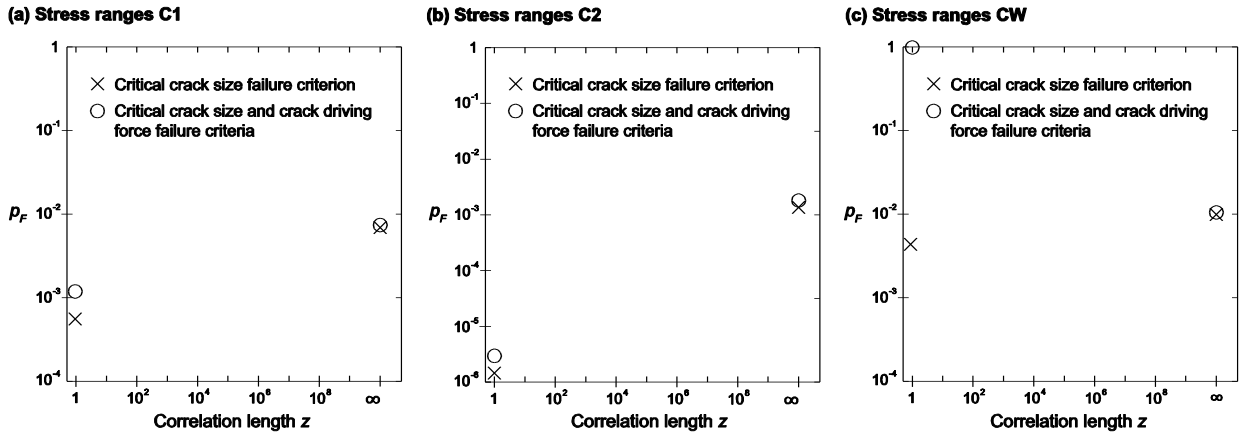

Fig. 15 *Probability of failure p_F versus correlation length z when applying either the critical crack size failure criterion alone or in combination with the crack driving force failure criteria. For $z = 1$, results are computed with SuS; for $z = \infty$, the MCS is applied .*

To understand the effect of the crack driving force failure criteria in the case of a random process model with a correlation length $z > 1$, some additional considerations are necessary.

Fig. 16 shows the empirical CDF of the maximum stress in a block, for the RV case and for the RP case with $z = 1$ and $z = 10^7$ (load model C1). The resulting CDF of case $z = 10^7$ is between the CDFs of the other two cases, which is to be expected given that those are the limit cases.

Fig. 17 depicts the empirical distribution of the crack depth a that causes failure according to the crack driving force failure criteria. These distributions correspond to the three CDFs of the maximum stresses given in Fig. 16. The critical crack depth applied in the critical crack size failure criterion is 21 mm. The mean crack depth at which the crack driving force failure occurs is close to the critical crack size criterion in all cases: it is 19 mm for the random variable load model and 18 mm and 15 mm for the random process models with $z = 10^7$ and $z = 1$ respectively. Therefore, the crack driving force failure criteria are reached just slightly before the critical crack size criterion, in particular since the crack growth rate increases strongly with crack size (see Fig. 12 and Fig. 13).

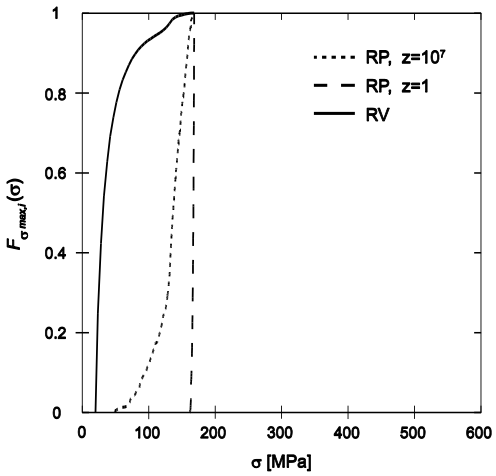

Fig. 16 *CDF of the maximum load for the random variable case (RV) and for the random process case with* $z = 1$ $(RP, z = 1)$ *and* $z = 10^7$ $(RP,\ z = 10^7)$*, evaluated for C1 with blocks of* $b = 10^4$ *cycles.*

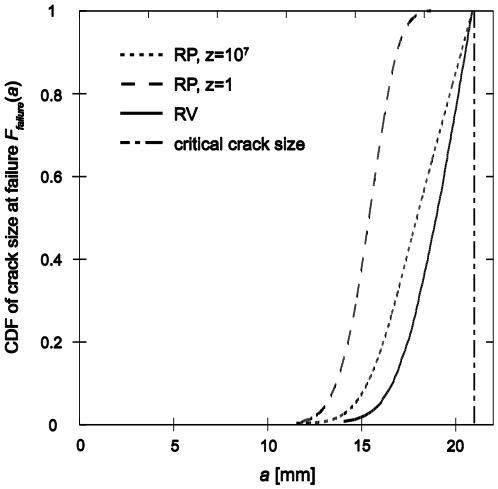

Fig. 17 *CDF of crack size at which unstable crack growth occurs for the random variable case (RV) and for the random process case with* $z = 1$ *(RP* $z = 1$*) and* $z = 10^7$ *(RP* $z = 10^7$*), evaluated for C1 with blocks of* $b = 10^4$ *cycles.*

From the above observations it follows that if the effect of the crack driving force failure criteria is small already for $z = 1$, it is reasonable to assume that it will be low also for values of $z > 1$. This is the case for load models C1 and C2. If the effect of the crack driving force failure criteria is significant for $z = 1$, additional computations, such as a cycle-by-cycle evaluation, may become necessary.

8 Discussion

The results of the numerical investigation point to the importance of accurately modeling the characteristics of the stress range process, in particular its correlation structure. In reliability analysis of structural components subject to fatigue, it has generally been assumed that the fatigue stress cycles are either fully correlated or uncorrelated. The results shown in Fig. 10 demonstrate that both these assumptions can overestimate the reliability. They indicate that the highest probability of failure occurs when the correlation length of the stress range process is of the same order of magnitude as the service life. This corresponds to structures that are subjected to a few distinct service conditions or mission types over their life-time. In these situations, the assumption of uncorrelated fatigue stress cycles leads to predictions of the probability of failure that may be several orders of magnitude too low. As shown in this paper, effective methods for considering the correlation structure of the stress range process in reliability analysis exist when using fracture mechanics based fatigue models.

It is pointed out that these results do not include retardation effects. When the retardation effect is relevant, the randomness of the load process has additional consequences, which are expected to be largest for small correlation lengths. Neither the mean approximation nor the block approximation can capture these effects. An exact reliability analysis appears to be possible only by combining the presented subset simulation based approach with the cycle-by-cycle evaluation, which however leads to large computational demands when evaluating high-cycle fatigue.

For the specific case study investigated in this paper, unstable crack growth (modeled by the crack driving force failure criteria) has only a limited effect on the reliability. Based on the authors' experiences, similar behavior is expected in many structures subject to high-cycle fatigue. The effect can be appraised by determining the probability distribution of the crack size at which unstable crack growth occurs (Fig. 17). If it can be ruled out that unstable crack growth plays a significant role, the reliability assessment is greatly simplified, as it becomes sufficient to evaluate the critical crack size failure criterion only. However, even if unstable crack growth has a limited effect on the reliability, it may still be necessary to consider it in case that not only the probability of failure but also the failure mode is of relevance. This can be the case for example in pipelines and pressure vessels where one needs to distinguish between failure by leakage and failure by burst.

The models presented in this work assume the presence of initial defects that behave like cracks. However, inclusion of crack nucleation and small crack growth into the reliability analysis would be straightforward, by combining the crack growth model with a crack nucleation model and a small crack growth model. For simplicity, the stress ratio was assumed constant throughout this paper. In analogy to the stress ranges, the stress ratios can be modeled through a random process, which would be correlated to the stress range process, and can be included in the reliability analysis following the presented approach.

9 Conclusion

Methods are presented for evaluating high cycle fatigue reliability under variable amplitude loading using fracture mechanics based crack growth models. The methods allow to explicitly account for the correlation structure of the load process: for stress range processes that are ergodic and have limited correlation, the mean approximation is suitable; for constant stress ranges, the random variable model is applicable; in all other cases, the proposed approach combining a load block model with the subset simulation provides a practical tool for assessing the reliability. The results of the numerical investigation show that the correlation structure of the stress range process has a significant influence on the estimated reliability. The probability of fatigue failure can varies by several orders of magnitude with varying correlation lengths.

Acknowledgements

We acknowledge the insightful comments of Johan Maljaars, Ton Vrouwenvelder and three anonymous reviewers on an earlier version of this manuscript. Iason Papaioannou is acknowledged for his support in the implementation of the subset simulation algorithm.

Annex A - Forman-Mettu model

The Forman-Mettu model provides a prediction of the fatigue threshold ΔK_{th} and the crack growth rate $\frac{\mathrm{d}x}{\mathrm{d}N}$, where x is alternatively the a or the c direction in the bi-dimensional crack growth model [33], [56]:

$$\Delta K_{th} = \frac{\Delta K_{th,0}}{\left[\frac{1-f}{[1-A_0](1-R)}\right]^{(1-C_{th}R)}} \tag{56}$$

$$\frac{\mathrm{d}x}{\mathrm{d}N} = C\left[\left(\frac{1-f}{1-R}\right)\Delta K_x\right]^m \cdot \frac{\left(1-\frac{\Delta K_{th}}{\Delta K_x}\right)^p}{\left(1-\frac{K_{x,max}}{K_{mat}}\right)^q}. \tag{57}$$

$\Delta K_{th,0}$ is the value of the fatigue threshold for $R = 0$. The empirical parameters p, q, m, C and C_{th} are obtained from the fitting to experimental data. ΔK_x is the stress intensity factor range in x-direction, $K_{x,max}$ the maximum value of the stress intensity factor. The functions f and A_0 depend on the stress range $\Delta\sigma$ and on the stress ratio R, on the constraint and on the material flow stress.

$$A_0 = (0.825 - 0.34 \cdot \alpha + 0.05 \cdot \alpha^2) \cdot \left[\cos\left(\frac{\pi}{2} \cdot \frac{\sigma_{max}}{\sigma_0}\right)\right]^{\frac{1}{\alpha}}$$

$$A_1 = (0.415 - 0.071 \cdot \alpha) \cdot \frac{\sigma_{\max}}{\sigma_0}$$

$$A_2 = 1 - A_0 - A_1 - A_3$$

$$A_3 = 2A_0 + A_1 - 1$$

$$f = \max\{R, A_0 + A_1 R + A_2 R^2 + A_3 R^3\}.$$

In this work, the stress σ_0 is considered equal to the cyclic yield stress $\sigma_{y,cycl}$. The ratio $\frac{\sigma_{max}}{\sigma_{0\,0}}$ is substituted with the ratio $\frac{K_{\max}}{K_0} = \frac{\beta\sigma_{max}}{\sigma_0}$, wherein K_0 is the stress intensity factor for a through crack in a panel. This approach has been demonstrated to successfully correlate the crack opening stresses for various specimen geometries [110][111].

References

[1] Suresh, S.. Fatigue of materials. Cambridge University Press; 1998.

[2] EN 1993-1-9 Eurocode 3: Design of steel structures - Part 1-9: Fatigue. 2005

[3] Dowling, N.. Fatigue failure prediction for complicated stress-strain histories. Journal of Materials 1972;7(1):71–87.

[4] ASTM E1049-85 Standard practices for cycle counting in fatigue analysis. 2011.

[5] Kaul, H.. Statistische Erhebungen über Betriebsbeanspruchungen von Flugzeugflügeln. Jahrbuch der Deutschen Luftfahrtforschung, Ergänzungsband 1938; 307–313.

[6] Gassner, E.. Festigkeitsversuche mit wiederholter Beanspruchung im Flugzeugbau Luftwissen (Strength tests under repeated loading for aeronautical engineering). 1939;6:61–64.

[7] Gassner, E.. Betriebsfestigkeit, eine Bemessungsgrundlage für Konstruktionsteile mit statistisch wechselnden Betriebsbeanspruchungen. Konstruktion 1954;6(3):97–104.

[8] Schütz, W.. A history of fatigue. Engineering Fracture Mechanics 1996;54(2):263–300.

[9] Tucker, L., Bussa, S.. The SAE cumulative fatigue damage test program. In: Wetzel, R., editor. Fatigue under complex loading - analyses and experiments. 1977, p. 1–54.

[10] Fash, J., Conle, F., Minter, G.. Analysis of irregular loading histories for the SAE biaxial fatigue program. In: Leese, G., D.Socie, editors. Multiaxial fatigue: analysis and experiments; vol. AE-14. Warrendale, PA: Society of Automotive Engineers; 1989, p. 33–59.

[11] Sonsino, C.. Fatigue testing under variable amplitude loading. International Journal of Fatigue 2007;29(6):1080–1089

[12] Heuler, P., Klätschke, H.. Generation and use of standardised load spectra and load-time histories. International Journal of Fatigue 2005;27:974–990

[13] Lardner, R.. Crack propagation under random loading. Journal of the Mechanics and Physics of Solids 1966;14(3):141–150

[14] Lardner, R.. Crack propagation under random loading - II. Journal of the Mechanics and Physics of Solids 1966;14(5):281–288

[15] Lardner, R.. A theory of random fatigue. Journal of the Mechanics and Physics of Solids 1967;15(3):205–221.

[16] Rau, I.. On fatigue-crack propagation under stationary random loading. International Journal of Engineering Science 1970;8(2):175–189.

[17] Head, A.. The growth of fatigue cracks. Philosophical Magazine 1953;44:925–938.

[18] Schijve, J.. Effect of load sequences on crack propagation under random and program loading. Engineering Fracture Mechanics 1971;5(2):269–280.

[19] Ditlevsen, O., Madsen, H.. Structural reliability methods. John Wiley & Sons; 1996.

[20] Anthes, R.J., Modified rainflow counting keeping the load sequence, International Journal of Fatigue 1997;19(7):529-535.

[21] Liu, P.L., De Kiureghian, A. Multivariate distribution models with prescribed marginal and covariances. Probabilistic Engineering Mechanics 1986;1(2):105-112.

[22] Lutes, L., Sarkani, S.. Random vibrations: Analysis of structural and mechanical systems. Oxford: Elsevier Butterworth - Heinemann; 2004.

[23] Rychlik, I.. Simulation of load sequences from rainflow matrices: Markov method. International Journal of Fatigue 1996;18(7):429-438.

[24] Johannesson, P., On rainflow cycles and the distribution of number of interval crossings by a Markov chain. Probabilistic Engineering Mechanics 2002;17(2):123–130.

[25] Straub, D.. Stochastic modeling of deterioration processes through dynamic bayesian networks. Journal of Engineering Mechanics 2009;135:1089 – 1099.

[26] Mattrand, C., Bourinet, J.. Random load sequences and stochastic crack growth based on measured load data. Engineering Fracture Mechanics 2011;78(17):3030–3048.

[27] Hohenbichler, M., Rackwitz, R.. Non-normal dependent vectors in structural safety. Journal of Engineering Mechanics 1981;107:6:1227–1238.

[28] Vanmarcke, E.. Random fields. Analysis and synthesis. Cambridge, MA: MIT Press; 1983.

[29] Newman, J.C., Raju, I.. Stress intensity factor equations for cracks in three- dimensional bodies subjected to tension and bending loads; vol. 2; chap. 9. Computational methods in the mechanics of fracture, edited by Atluri S.N.; Elsevier Science Publishers B.V.; 1986,.

[30] Černý, I., The use of DCPD method for measurement of growth of cracks in large components at normal and elevated temperatures. Engineering Fracture Mechanics 2004:71:837-848.

[31] BS 7910 Guide to methods for assessing the acceptability of flaws in metallic structures. 2005.

[32] Righiniotis, T.D., Chryssanthopoulos, M.K.. Fatigue and fracture simulation of welded bridge details through a bi-linear crack growth law. Structural Safety 2004;26(2):141–158.

[33] Forman, R., Mettu, S.. Behavior of surface and corner cracks subjected to tensile and bending loads in a Ti-64Al-4V alloy. In: Ernst, H., Saxena, A., McDowell, D., editors. Fracture Mechanics: Twenty-Second Symposium; vol. I of ASTM STP 1131. American Society for Testing and Materials; 1992, p. 519–546.

[34] Suresh, S.. Fatigue of materials. Cambridge University Press; 1998.

[35] Dominguez, J., Zapatero, J., Pascual, J.. Effect of load histories on scatter of fatigue crack growth in aluminium alloy 2024-T351. Engineering Fracture Mechanics 1997;56(65-76).

[36] Miranda, A., Meggiolaro, M., Castro, Z., Martha, L., Bittencourt, T.. Fatigue life and crack path predictions in generic 2D structural components. Engineering Fracture Mechanics 2003;70(10):1259–1279.

[37] Elber, W.. Fatigue crack closure. Engineering Fracture Mechanics 1970;2.

[38] Elber, W.. The significance of crack closure. In: Damage Tolerance in Aircraft Structure ASTM/STP 486. 1971,230-242.

[39] Wheeler, O.E.. Spectrum loading and crack growth. Journal of basic engineering - Transaction ASME 1972;94:181–186.

[40] Willenborg, J.D.. Engle, R.M., Wood, H.A., A crack growth retardation model using an effective stress concept. Tech. Rep. AFFDL-TM-FBR-71-1; Airforce Flight Dynamics Lab; 1971.

[41] Newman, J.. A crack closure model for predicting fatigue crack growth under aircraft spectrum loading. In: Hudson, J.C.C., editor. Methods and models for predicting fatigue crack growth under random loading. ASTM STP 748; 1981,53-84.

[42] Donald, K., Paris, P.C.. An evaluation of ΔKeff estimation procedures on 6061- T6 and 2024-T3 aluminium alloys. International Journal of Fatigue 1999;21.

[43] Murakami, Y.. Stress intensity factor handbook. Oxford: Pergamon Press; 1987.

[44] Wu, X., Carlsson, A.. Weight functions and stress intensity factor solutions. Oxford, UK: Pergamon Press; 1991.

[45] Fett, T., Munz, D.. Stress intensity factors and weight functions. In: Computational Mechanics Publications. Southtampton; 1997.

[46] Tada, H., Paris, P., Irwin, G.. The stress analysis of cracks handbook. 3rd ed.; New York: ASME Press; 2000.

[47] Gdoutos, E., Hatzitrifon, N.. Growth of three-dimensional cracks in finite thickness plates. Engineering Fracture Mechanics 1987;26(6):883–895.

[48] Schöllmann, M., Fulland, M., Richard, H.. Development of a new software for adaptive crack growth simulations in 3D structures. Engineering Fracture Mechanics 2003;70(2):249–268.

[49] Moslemi, H., Khoei, A.. 3D adaptive finite element modeling of non- planar curved crack growth using the weighted superconvergent patch recovery method. Engineering Fracture Mechanics 2009;76(11):1703–1728.

[50] Boljanovi´c, S., Maksimovi´c, S.. Analysis of the crack growth propagation under mixed-mode loading. Engineering Fracture Mechanics 2011;78(12):1565– 1576.

[51] Zerbst, U., Schödel, M., Webster, S., Ainsworth, R.. Fitness-for-service. Fracture assessment of structures containing cracks. Elsevier Science; 2007.

[52] Straub, D.. Generic approaches to risk based inspection planning for steel structures. Ph.D. thesis; Swiss Federal Institute of Technology Zürich; 2004.

[53] Lin, X.B., Smith, R.A.. Finite element modelling of fatigue crack growth of surface cracked plates,

Part I: The numerical technique,. Engineering Fracture Mechanics 1999;63:503–522.

[54] Newman, J.C., Brot, A., Matias, C.. Crack-growth calculations in 7075- T7351 aluminum alloy under various load spectra using an improved crack- closure model. Engineering Fracture Mechanics 2004;71:2347–2363.

[55] Altamura, A., Beretta, S.. Reliability assessment of hydraulic cylinders considering service loads and flaw distribution. International Journal of Pressure Vessels and Piping 2012;98:76–88.

[56] Harter, J.A.. AFGROW users guide and technical manual. Tech. Rep.; US air force reseach laboratory technical report AFRL-VA-WP-TR-2006-XXXX; Air vehicle directorate, 2790 D Street, Ste 504; 2006.

[57] Maljaars, J., Steenbergen, H., Vrouwenvelder, A.. Probabilistic model for fatigue crack growth and fracture of welded joints in civil engineering structures. International Journal of Fatigue 2012;38:108–117.

[58] Papoulis, A., Pillai, S.. Probability, random variables and stochastic processes. McGraw Hill; 2002.

[59] Hudson, C.. A root mean square approach for predicting fatigue crack growth under random loading. In: Chang, J.B., Hudson, C., editor. Methods and models for predicting fatigue crack growth under random loading. ASTM STP 748; American Society for Testing and Materials; 1981, p. 41–52.

[60] Wirsching, P., Chen, Y.. Considerations of probability-based fatigue design for marine structures. Marine Structures 1988;1(1):23–45.

[61] Forman, R., Shivakumar, V., Mettu, S., Newman, J.. Fatigue crack growth computer program NASGRO - version 3.0. Tech. Rep.; NASA; Johnson Space Center, Houston, Texas; 2000.

[62] Zerbst, U., Vormwald, M., Andersch, C., Mädler, K., Pfuff, M.. The development of a damage tolerance concept for railway components and its demonstration for a railway axle. Engineering Fracture Mechanics 2005;72:209–239.

[63] Beretta, S., Carboni, M.. Experiments and stochastic model for propagation lifetime of railway axles. Engineering Fracture Mechanics 2006;73(17):2627– 2641.

[64] Sander, M., Richard, H. A., Investigations on fatigue crack growth under variable amplitude loading in wheelset axles. Engineering Fracture Mechanics 2011;78:754–763.

[65] Moore, H., Kommers, J.. The fatigue of metals. New York: McGraw Hill; 1927.

[66] Virkler, D., Hillberry, B., Goel, P.. The statistical nature of fatigue crack propagation. Journal of Engineering Materials and Technology 1979;101(2):148–153.

[67] Ortiz, K., Kiremidjian, A.. Stochastic modeling of fatigue crack growth. Engineering Fracture Mechanics 1988;29(3):317–334.

[68] Yang, J.N., Manning, S.D.. A simple second order approximation for stochastic crack growth analysis. Engineering Fracture Mechanics 1996;53(5):677–686.

[69] Tsurui, A., Ishikawa, H.. Application of the Fokker-Planck equation to a stochastic fatigue crack growth model. Structural Safety 1986;4(1):15–29.

[70] Ishikawa, H., Tsurui, A.. A stochastic model of fatigue crack growth in consideration of random propagation resistance. Transaction of JSME 1984;50:1309– 1315.

[71] Ishikawa, H., Tanaka, H., Wakasa, S.. A stochastic crack growth model with propagation resistance as a random field. In: Rackwits, R., Augusti, G., Borri, A., editors. Reliability and optimization of structural systems. London, UK: Chapman and Hall; 1995,.

[72] Xing, J., Zhong, Q.P., Hong, Y.J.. A simple log normal random process approach of the fatigue crack growth considering the distribution of initial crack size and loading condition. International Journal of Pressure Vessels and Piping 1997;74(1):7–12.

[73] Chen, C., Liu, C., Chen, J., Yu, A., Hsu, H.. The effects of material variations on aircraft inspection schedules based on stochastic crack growth model. International Journal of Fatigue 2008;30:861–869.

[74] Lauschmann, H.. A stochastic model of fatigue crack growth in heterogeneous material. Engineering Fracture Mechanics 1987;26:707–728.

[75] Chiaki, I., Misawa, T.. A stochastic model for fatigue crack propagation with random propagaton resistance. Engineering Fracture Mechanics 1988;31:95-104.

[76] Vrouwenvelder, A., Spatial correlation aspects in fatigue models, eds. Ditlevsen O. Friis Hansen P., Proceedings of the two parts workshop, August 2004, 2005 ISBN 87-89502,

[77] Vrouwenvelder, A., Fatigue modelling according to the JCSS probabilistic model code, In Aspects of Structural Reliability in Honor of R. Rackwitz, Eds. Faber M., Vrouwenvelder A., Zilch K., 2007, ISBN 978-3-8316-0752-5

[78] Provan, J. W., Sih, G. C., Probabilistic fracture mechanics and reliability. Kluwer Academic Publishers; 1986.

[79] Kozin, F., Bogdanoff, J.L.. A critical analysis of some probabilistic models of fatigue crack growth. Engineering Fracture Mechanics 1981;14:59-89.

[80] Kozin, F., Bogdanoff, J.L.. On the probabilistic modeling of fatigue crack growth. Engineering Fracture Mechanics 1983;18:623-632.

[81] Lin, Y., Yang, J.. On statistical moments of fatigue crack propagation. Engineering Fracture Mechanics 1983;18(2):243–256.

[82] Lin, Y., Yang, J.. A stochastic theory of fatigue crack propagation. AIAA Journal 1985;23(1):117–124.

[83] Tanaka, H., Tsurui, A.. Reliability degradation of structural components in the process of fatigue crack propagation under stationary random loading. Engineering Fracture Mechanics 1987;27:501–516.

[84] Rocha, M., Schüeller, G.. A probabilistic criterion for evaluating the goodness of fatigue crack growth models. Engineering Fracture Mechanics 1996;53(5):707–731.

[85] Wu, W.F., Ni, C.C.. A study of stochastic fatigue crack growth modeling through experimental data. Probabilistic Engineering Mechanics 2003;18:107-118.

[86] Zheng, R., Ellingwood, B.. Stochastic fatigue crack growth in steel structures subject to random loading. Structural Safety 1998;20(4):303–323.

[87] Yang, J., Salivar, G., Annis, C.. Statistical modeling of fatigue-crack growth in a nickel-base superalloy. Engineering Fracture Mechanics 1983;18(2):257– 270.

[88] Sobczyk, K., Spencer, B.F. Jr.. Random fatigue: from data to theory. New York: Academic Press; 1992.

[89] Lidiard, A.B.. Probabilistic fracture mechanics. In: Fracture mechanics, current status, future prospects. Pergamon Press; 1979,.

[90] Engesvik, K.M.. Moan, T., Probabilistic analysis of the uncertainty in the fatigue capacity of welded joints.; Engineering Fracture Mechanics1983:18(4):743-762.

[91] Varanasi, S.R., Whittaker, I.C.. Structural reliability prediction method considering crack growth and residual strength. In: Fatigue crack growth under spectrum loads. ASTM STP 595; 1976,.

[92] Annis, C.. Probabilistic life prediction isn't as easy as it looks. In: Johnson, W., B.M. Hillberry, E., editors. Probabilistic aspects of life prediction, ASTM STP-1450. West Conshohocken, PA: ASTM International; 2003.

[93] Radhakrishnan, V.M.. Quanitfying the parameters in fatigue crack propagation. Engineering Fracture Mechanics 1980;13:129–141.

[94] Dolinski, K.. Stochastic loading and material inhomogeneity in fatigue crack propagation. Engineering Fracture Mechanics 1986;25(5-6):809-818.

[95] Sobczyk, K.. Modelling of random fatigue crack growth. Engineering Fracture Mechanics 1986;24(4):609–623.

[96] Rackwitz, R.. Reliability analysis—a review and some perspectives. Structural Safety 2001;23:365–395.

[97] Melchers, R.. Structural reliability analysis and prediction. John Wiley & Sons; 2002.

[98] Kocak, M., Webster, S., Janosch, J., Ainswort, R.A., Koers, R.. Fitness for service procedure. FITNET; 2006.

[99] Harrison, R., Loosemore, K., Milne, I.. Assessment of the integrity of structures containing defects. Tech. Rep. R/H/R6; CEGB; 1976.

[100] Milne, I., Ainsworth, R., Dowling, A.R., Stewart, A.. Assessment of the integrity of structures containing defects. Intenational Journal of Pressure Vessels and Pipings, 1986;32(1-4):3-104.

[101] Rackwitz, R., Flessler, B.. Structural reliability under combined random load sequences. Computers and Structures 1978;9(5):489–494.

[102] Rao, S.. Reliability based design. Mcgraw-Hill; 1992.

[103] Hasofer, A., Lind, N.. An exact and invariant first order reliability format. Journal of Engineering Mechanics 1974;100(1):111–121.

[104] Au, S., Beck, J.. Estimation of small failure probabilities in high dimensions by subset simulation. Probabilistic Engineering Mechanics 2001;16:263–277.

[105] Anderson, T.. Fracture mechanics: fundamentals and applications. 2nd ed.; Boca Raton: CRC Press; 1995.

[106] Cristea, M., Beretta, S., Altamura, A.. Fatigue limit assessment on seamless tubes in presence of inhomogeneities: small crack model vs. full scale testing experiments. International Journal of Fatigue 2012;41:150–157.

[107] EN 10305-1 Steel tubes for precision applications. Technical delivery conditions. Seamless cold drawn tubes. 2010.

[108] EN 10297-1 Seamless circular steel tubes for mechanical and general engineering purposes. Technical delivery conditions. Non alloy and alloy steel tubes. 2003.

[109] Dominguez, J., Zapatero, J., Moreno, B.. A statistical model for fatigue crack growth under random loads including retardation effects. Engineering Fracture Mechanics 1999;62:351–369.

[110] McClung, R., Sehitoglu, H.. On the finite element analysis of fatigue crack closure-1. basic modelling issues. Engineering Fracture Mechanics 1989;33(22A):237–252.

[111] McClung, R.. The influence of applied stress, crack length and stress intensity factor on crack closure. Metallurgical Transactions A 1991;22A(33):1559–1571.